Epidemics 39 (2022) 100560

Contents lists available at ScienceDirect

Epidemics

journal homepage: www.elsevier.com/locate/epidemics

A wastewater-based epidemic model for SARS-CoV-2 with application to three Canadian cities

Shokoofeh Nourbakhsh [a,1], Aamir Fazil [a], Michael Li [a], Chand S. Mangat [b], Shelley W. Peterson [b], Jade Daigle [b], Stacie Langner [b], Jayson Shurgold [c], Patrick D'Aoust [d], Robert Delatolla [d], Elizabeth Mercier [d], Xiaoli Pang [e,f], Bonita E. Lee [g], Rebecca Stuart [h], Shinthuja Wijayasri [h,i], David Champredon [a,*,1]

[a] Public Health Risk Sciences Division, National Microbiology Laboratory, Public Health Agency of Canada, Guelph, ON, Canada
[b] One Health Division, National Microbiology Laboratory, Public Health Agency of Canada, Winnipeg, MB, Canada
[c] Antimicrobial Resistance Division, Infectious Diseases Prevention and Control Branch, Public Health Agency of Canada, Ottawa, ON, Canada
[d] University of Ottawa, Department of Civil Engineering, Ottawa, ON, Canada
[e] Public Health Laboratory, Alberta Precision Laboratory, Edmonton, AB, Canada
[f] Department of Laboratory Medicine and Pathology, University of Alberta, Edmonton, AB, Canada
[g] Department of Pediatrics, University of Alberta, Edmonton, AB, Canada
[h] Toronto Public Health, Toronto, ON, Canada
[i] Canadian Field Epidemiology Program, Emergency Management, Public Health Agency of Canada, Canada

ARTICLE INFO

Keywords:
Epidemic model
SARS-CoV-2/COVID-19
Environmental surveillance
Wastewater

ABSTRACT

The COVID-19 pandemic has stimulated wastewater-based surveillance, allowing public health to track the epidemic by monitoring the concentration of the genetic fingerprints of SARS-CoV-2 shed in wastewater by infected individuals. Wastewater-based surveillance for COVID-19 is still in its infancy. In particular, the quantitative link between clinical cases observed through traditional surveillance and the signals from viral concentrations in wastewater is still developing and hampers interpretation of the data and actionable public-health decisions. We present a modelling framework that includes both SARS-CoV-2 transmission at the population level and the fate of SARS-CoV-2 RNA particles in the sewage system after faecal shedding by infected persons in the population. Using our mechanistic representation of the combined clinical/wastewater system, we perform exploratory simulations to quantify the effect of surveillance effectiveness, public-health interventions and vaccination on the discordance between clinical and wastewater signals. We also apply our model to surveillance data from three Canadian cities to provide wastewater-informed estimates for the actual prevalence, the effective reproduction number and incidence forecasts. We find that wastewater-based surveillance, paired with this model, can complement clinical surveillance by supporting the estimation of key epidemiological metrics and hence better triangulate the state of an epidemic using this alternative data source.

1. Introduction

Wastewater has been used previously for monitoring of a wide range of behavioural, socio-economic and biological markers including: medical and illicit drugs Feng et al. (2018); Zuccato et al. (2008, 2005); antibiotic and antimicrobial resistance Christou et al. (2017); Rizzo et al. (2013); Laht et al. (2014); and industrial pollutant chemicals Rousis et al. (2017, 2016). Spatial and temporal screening of the wastewater collection system or "sewershed" can provide qualitative and quantitative information on the marker of interest within the population in a given sewer catchment contributing to the wastewater. The wastewater data when used as an index of disease burden can be incorporated into traditional surveillance tools for monitoring disease prevalence that is purposeful, economical and action-oriented for public health Gawlik et al. (2021). Wastewater-based surveillance (WBS) has also proven to be a low-cost and non-invasive tool for the management of infectious

* Corresponding author.
E-mail address: david.champredon@canada.ca (D. Champredon).
[1] contributed equally

https://doi.org/10.1016/j.epidem.2022.100560
Received 16 August 2021; Received in revised form 7 March 2022; Accepted 3 April 2022
Available online 8 April 2022

disease pathogens such as norovirus Lun et al. (2018); Fioretti et al. (2018) and poliovirus Asghar et al. (2014); Duintjer Tebbens et al. (2017); Brouwer et al. (2018) where viral concentration in wastewater served to supplement clinical surveillance. Since the start of the COVID-19 pandemic, SARS-CoV-2 RNA has been detected and quantified in sewage in many locations worldwide Naughton (2020) and was employed successfully in correlating the concentration of SARS-CoV-2 in wastewater to clinical cases reported in the sewershed Medema et al. (2020); Ahmed et al. (2020); Wurtzer et al. (2020); Peccia et al. (2020); La Rosa et al. (2020); Larsen and Wigginton (2020); Randazzo et al. (2020); D'Aoust et al. (2021); Hata et al. (2021). In some instances of institutional surveillance, the leading wastewater signal (measured as SARS-CoV-2 RNA concentration in wastewater) compared to the clinical reports provided an early sign for the introduction or resurgence of COVID-19 into a community Gibas et al. (2021); Peiser (2020); Paglinawan (2020); D'Aoust et al. (2021) enabling rapid deployment of public health response and mitigation efforts.

Despite numerous successes with wastewater-based surveillance during the pandemic, utilizing wastewater surveillance data as a public-health tool for quick response remains challenging for some jurisdictions, especially at the municipal level National Institute for Public Health Netherlands (2021); Public Health Ottawa (2021a). A major hurdle is the lack of a quantitative framework to assess and interpret the wastewater data generated and to translate that into public health action Public Health Ontario (2021b); WHO (2020). The common practice is to use the detection of SARS-CoV-2 in wastewater as a signal for COVID-19 (re)introduction in a community and/or perform trend analysis in parallel with clinical surveillance of COVID-19. At the time of this manuscript, it is generally not recommended to use SARS-CoV-2 WBS for direct inference of key epidemiological indicators such as prevalence of active infections Public Health Ontario (2021b); WHO (2020); Medema et al. (2020); Foladori et al. (2020).

Public health response guided by SARS-CoV-2 levels in wastewater is currently hindered by a lack of structured interpretive criteria, which is at present obscured by the inherent complexity and variation imparted by diverse sewersheds and their contributing populations Li et al. (2021); Zhu et al. (2021); Rabson (2021). Sources of data variability includes individual's shedding dynamics, sampling frequency of wastewater, non-standardized laboratory methods, sewershed-specific viral degradation and signal attenuation during its journey from the site of faecal shedding (and potentially from urinary or sputum deposit Jones et al. (2020); Wang et al. (2020)) to the sampling point. Attenuation of RNA signal in wastewater involves several factors, such as dilution in municipal wastewater constituents (e.g., storm water effects in combined sewers and infiltration effects in both combined and separated sewers), RNA degradation (e.g., due to household detergents and industrial wastewaters) and viral degeneration in the harsh wastewater environment due to temperature, bioactive chemicals, pH, etc. Solids sedimentation and resuspension may also play a key role in the transportation and decay of SARS-CoV-2 RNA because of the hydrophobic characteristics of the viral envelope and its strong associations to solids Gundy et al. (2009); Foladori et al. (2020). In addition, concentration methods for detection enhancement and minimization of inhibitory substances of molecular tests can result in some loss of the viral target Kitajima et al. (2020); Michael-Kordatou et al. (2020).

Here, we present a modelling framework that attempts to link quantified SARS-CoV-2 levels in wastewater with estimates of infections in the population within the sewershed, and to support policy decisions. The model incorporates both the viral transmission within the population via a standard epidemiological SEIR-like model ("Susceptible - Exposed - Infectious - Recovered") Anderson and May (1991) and the fate of SARS-CoV-2 in wastewater using a simplified hydrological transport framework. To illustrate potential applications, we fit our model to WBS data and traditional clinical reports gathered from six wastewater treatment plants (WWTPs) located in three Canadian cities (Edmonton, Ottawa and Toronto) and provide wastewater-informed estimates of key epidemiological metrics. We also perform exploratory simulations to investigate how the wastewater signal can be mechanistically associated with clinical surveillance of COVID-19.

2. Methods

We develop a mathematical model that mechanistically describes both the transmission at the population level ("above ground") and the concentration of SARS-CoV-2 in wastewater as a result of faecal shedding from the infected individuals ("below ground").

2.1. Transmission between individuals

To model SARS-CoV-2 transmission in the population, we use a SEIR-type epidemiological model. The disease progression of individuals is captured through several compartments that reflect their epidemiological states and disease outcomes (Table 1). Individuals can be susceptible (S); exposed (infected but not yet infectious, E); symptomatically infected who will later become hospitalized (J) or recovered without hospitalization during active COVID-19 (I); asymptomatically infected (A); hospitalized (H); those recovered and no longer infectious but still shedding virus in faeces (Z); fully recovered and permanently immune but not shedding anymore (R) and deceased (D). We ignore any migration movements, so at any given time the total population is constant and equal to $N = S + E + J + I + A + H + Z + R + D$. Infection occurs at a time-dependent transmission rate β_t between infectious (states I, J or A) and susceptible individuals (S). Once infected, susceptible individuals enter the latent (non-infectious) state (E) for an average duration of $1/\epsilon$ days, where no faecal shedding occurs. A proportion α of all infections are asymptomatic. A fraction h of symptomatic individuals are hospitalized (H) for an average duration of $1/\ell$ days and for those, the COVID-19-associated mortality is δ. After their infectious period ends, patients enter the post-infection shedding state Z where SARS-CoV-2 faecal shedding still occurs for $1/\eta$ days on average. The exposed (E), infectious (A, I and J) and post-infection shedding (Z) states are modelled with a series of sub-compartments in order to have their

Table 1
Description of the model's compartments and parameters for the SARS-CoV-2 transmission within population and disease outcome.

Symbole	Definition
S	susceptibles
E_k	exposed susceptibles but not infectious in kth subcompartment
A_k	asymptomatic infectious cases in kth subcompartment
I_k	symptomatic infectious cases in kth subcompartment
J_k	symptomatic infectious cases in kth subcompartment who later admits to hospital
Z_k	non-infectious cases but fecal shedding SARS-CoV-2 RNA in kth subcompartment
H	hospitalized patients
R	recovered cases
D	deceased cases
β_t	time-dependent transmission rate (per contact)
$1/\varepsilon_k$	ave. latency time in kth subcompartment (days)
$1/\nu_k$	ave. duration in kth subcompartment among symptomatics (days)
$1/\mu_k$	ave. duration in kth subcompartment among symptomatics admit to hospital (days)
$1/\theta_k$	ave. duration in kth subcompartment among asymptomatics (days)
$1/\eta_k$	ave. duration in kth subcompartment of shedding after infectiousness (days)
$1/\ell$	ave. length of stay in a hospital (days)
n_E	total number of subcompartments in E state
n_I	total number of subcompartments in I state
n_J	total number of subcompartments in J state
n_A	total number of subcompartments in A state
n_Z	total number of subcompartments in Z state
α	proportion of exposed cases that are asymptomatic
h	proportion of symptomatic cases that need hospital admission
δ	proportion of deceased individuals among hospitalized patients

respective sojourn time gamma-distributed Wearing et al. (2005); He et al. (2020); Li et al. (2020).

The transmission dynamics are represented by the system of differential equations 1a-1n and illustrated in Fig. 1.

$$\dot{S} = -\beta_t S(\widetilde{A} + \widetilde{I} + \widetilde{J})/\mathrm{N} \tag{1a}$$

$$\dot{E}_1 = \beta_t S(\widetilde{A} + \widetilde{I} + \widetilde{J})/\mathrm{N} - \mathrm{n_E}\varepsilon \mathrm{E_1} \tag{1b}$$

$$\dot{E}_k = n_E \varepsilon (E_{k-1} - E_k) 2 \le k \le n_E \tag{1c}$$

$$\dot{A}_1 = \alpha \varepsilon E_{n_E} - n_A \theta A_1 \tag{1d}$$

$$\dot{A}_k = n_A \theta (A_{k-1} - A_k) 2 \le k \le n_A \tag{1e}$$

$$\dot{I}_1 = (1-h)\,(1-\alpha)\varepsilon E_{n_E} - n_I \nu I_1 \tag{1f}$$

$$\dot{I}_k = n_I \nu (I_{k-1} - I_k) 2 \le k \le n_I \tag{1g}$$

$$\dot{J}_1 = h(1-\alpha)\varepsilon E_{n_E} - n_J \mu J_1 \tag{1h}$$

$$\dot{J}_k = n_J \mu (J_{k-1} - J_k) 2 \le k \le n_J \tag{1i}$$

$$\dot{H} = n_J \mu J_{n_J} - \ell H \tag{1j}$$

$$\dot{Z}_1 = n_I \nu I_{n_I} + n_A \theta A_{n_A} - n_Z \eta Z_1 \tag{1k}$$

$$\dot{Z}_k = n_Z \eta (Z_{k-1} - Z_k) \qquad 2 \le k \le n_Z \tag{1l}$$

$$\dot{R} = n_Z \eta Z_{n_Z} + (1-\delta)\ell H \tag{1m}$$

$$\dot{D} = \delta\, \ell H \tag{1n}$$

where $\widetilde{A} = \xi \sum_{k=1}^{n_A} \phi_k A_k$, $\widetilde{I} = \sum_{k=1}^{n_I} \psi_k I_k$ and $\widetilde{J} = \sum_{k=1}^{n_J} \psi_k J_k$. We use the dot notation to symbolize derivation with respect to time (e.g., $\dot{S} = dS/\mathrm{dt}$).

The parameters ϕ_k and ψ_k are multiplicative adjustments to the baseline transmission rate β_t to represent the infectious profile during the course of infection. The values for ϕ_k and ψ_k were chosen to represent the best estimate of the temporal infectiousness profile (hence their values are distinct, not constant) given the different results published (see Appendix A-2 and A-3 for details). The parameter ξ models the relative infectiousness of asymptomatic cases compared to symptomatic ones. The effective reproduction number of this model is (see Appendix A-4 for details on its calculation):

$$\mathscr{R}_t = \beta_t \left(\alpha\xi \frac{1}{\theta} + (1-h)(1-\alpha)\frac{1}{\nu} + h(1-\alpha)\frac{1}{\mu}\frac{\sum_{k=1}^{n_J}\psi_k}{n_I} \right) \frac{S_t}{N} \tag{2}$$

2.2. SARS-CoV-2 viral concentration in wastewater

2.2.1. Deposited viral concentration

The daily concentration of SARS-CoV-2 in wastewater is directly calculated from the total number of individuals that are actively shedding into the sewage system. SARS-CoV-2 faecal shedding varies according to the infected individual's clinical state and disease outcomes. Depending on the disease progression, infected individuals shed a variable amount of SARS-CoV-2 while they are in the shedding states (A, I, J and Z). We make the simplifying assumption that hospitalized patients (H)–assumed mostly bedridden and a small fraction of the shedding population–do not contribute to faecal shedding. Moreover, we assume that individuals in their latent period (E) do not contribute to faecal shedding: if they are not shedding enough through the respiratory tract be infectious, they may not shed significantly through the faecal route too.

The total concentration of SARS-CoV-2 RNA entering the wastewater at time t is given by

$$W^*(t) = \omega \times \left(\sum_{k=1}^{n_J} \lambda_k J_k(t) + \sum_{k=1}^{n_I} \lambda_k I_k(t) + \xi \sum_{k=1}^{n_A} \lambda_k A_k(t) + \sum_{k=1}^{n_Z} \lambda_k Z_k(t) \right) \tag{3}$$

The parameters λ_k, represent SARS-CoV-2 faecal shedding dynamics per capita when the infected individual is in any of the epidemiological

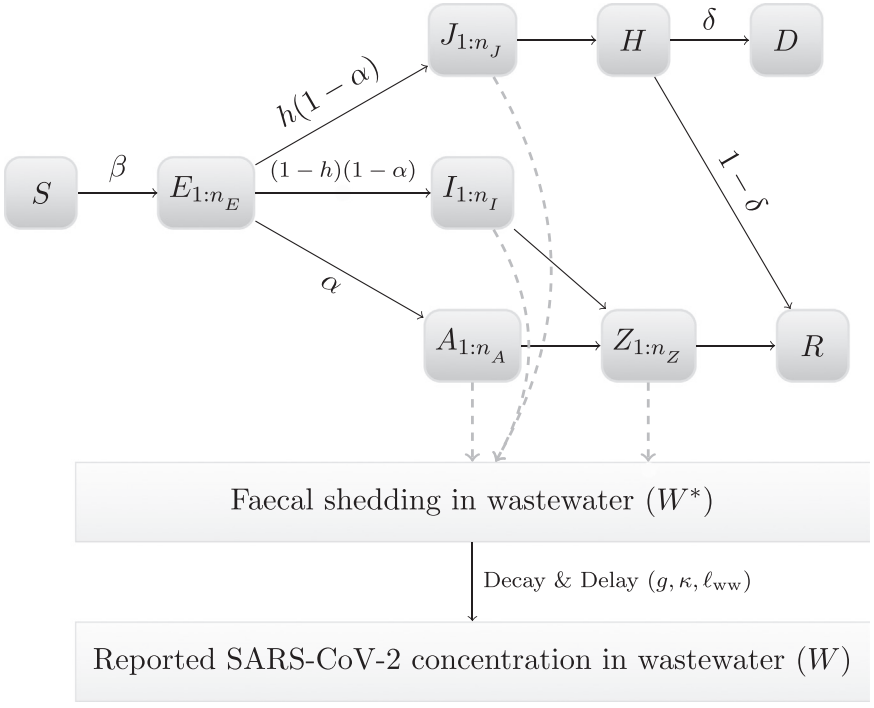

Fig. 1. Diagram of compartmental model. See main text for a description of the epidemiological states. The notation 1: $n_\bullet$ indicates a modelling using $n_\bullet$ sub-compartments to obtain a gamma-distributed sojourn time in the associated epidemiological state.

states (i.e., I, J, A and Z). Given the current lack of observational data, we used the same parameters λ_k for all epidemiological states. Values for λ_k were set at mid-range values of published studies (see Appendix A-3). Note that we assume the same reduction in faecal shedding as in respiratory shedding for asymptomatic cases (parameter ξ). The parameter ω implies that our model can only determine up to a constant the concentration of SARS-CoV-2 in wastewater Brouwer et al. (2018), even if the limit of detection of the assay is known. This reflects our current inability to quantify the various complex processes that affect the concentration, from patients' shedding to the concentration measured in laboratories (e.g., frequency and timing of sampling, RNA degradation in the sewer system, recovery efficiency of assays).

2.2.2. RNA transport and sampled viral concentration

We use a simple advection-dispersion-decay model to simulate the fate of SARS-CoV-2 along its journey in wastewater from the shedding points to the sampling site. This model is a combination of an exponential viral decay Ahmed et al. (2020) and a τ-day dispersed plug-flow function, $g(\tau)$, representing all possible hydrodynamic processes (e.g., dilution, sedimentation and resuspension) that leads to RNA degradation as well as decrease and delay of signal at the time of sampling. The dispersed plug-flow $g(\tau)$ acts as a transformation function, which reshapes the initial deposited concentration, W^* , into a delayed viral distribution over τ days as a result of the transit of SARS-CoV-2 in the sewer system. Hence, we defined the sampled viral concentration at time t as:

$$W_{\text{samp}}(t) = \int_0^t W * (t-\tau)\, g(\tau)\, e^{-\kappa\tau} \mathrm{d}\tau, \tag{4}$$

where κ is the daily first-order decay rate of SARS-CoV-2 due to the harsh, complex and bioactive environment of wastewater. Because of the lack of decay-specific data for any of our sampling locations, we naively set its value based on the literature Ahmed et al. (2020); Silverman and Boehm (2020) at $\kappa = 0.18\ \text{day}^{-1}$ for all locations. The SARS-CoV-2 RNA concentration entering the sewage system daily is modelled as a single hydrodynamic pulse per day and the plug-flow function, g, is obtained by the analytical solution of the axial dispersed plug flow differential equation Kayode Coker (2001). We then re-parametrize the analytical solution with the mean delay time $\overline{\tau}$ and its standard deviation σ into a Gaussian distribution

$$g(\tau) = \frac{1}{\sqrt{2\pi}\sigma} \exp\left(-\frac{(\tau-\overline{\tau})^2}{2\sigma^2} \right). \tag{5}$$

Note that our advection-dispersion-decay model of the RNA transport is not a spatial model and the physical/biochemical characteristics of each WWTPs and their unique wastewater matrix are not modelled in Equation 4 and Equation 5. The simple dispersed plug flow model (Equation 5) only modelled the average transit time of the viral particles ($\overline{\tau}$) in a given sewershed influenced by the unknown viral chemical partitioning and hydrodynamical sedimentation. See Appendix A-5 for more details.

2.2.3. Wastewater reported sample

The sample transportation, laboratory processing time and reporting lags, introduce reporting delays of RNA concentration in wastewater. Hence, we define the reported wastewater concentration as

$$W(t) = W_{\text{samp}}(t - \ell_{\text{ww}}), \tag{6}$$

where ℓ_{ww} is the reporting lag between wastewater sampling and concentration report after laboratory analysis. (Note that the reporting delay of the wastewater measurement is independent from the delay caused by the transport of RNA particles in the sewer system as defined in Equation 4).

2.3. Clinical reported cases

We also model surveillance data derived from laboratory confirmed and clinically diagnosed COVID-19 cases, acknowledging that instantaneous identification and complete reporting after initial infection is not possible. We assume that a fraction ρ of symptomatic incidence is reported with a lag of a ℓ_{clinical} days from the time of infection. If $i(t)$ is the total incidence at time t, we define the number of clinical cases reported at time t as:

$$C(t) = \rho\,(1-\alpha)\, i(t - \ell_{\text{clinical}}), \tag{7}$$

2.4. Wastewater and clinical surveillance data

We apply our modelling framework to data sets from six wastewater sampling sites located in three Canadian cities: Edmonton (Alberta), Ottawa (Ontario) and Toronto (Ontario). Sampling sites are the following municipal WWTPs (abbreviation / approximate population served): Gold Bar in Edmonton (EGB / 900,000); Robert O. Pickard Environmental Centre in Ottawa (OTW / 1,000,000 City of Ottawa (2021)); Toronto Ashbridges Bay (TAB / 1,603,700 Toronto Water (2021a)); Toronto Humber (THU / 685,000 Toronto Water (2021b)); Toronto Highland Creek (THC / 533,000 Toronto Water (2021c)); and Toronto North Toronto (TNT / 252,530 Statistics Canada (2016)).

2.4.1. Data collection

Wastewater samples were collected approximately two (Edmonton and Toronto) to seven (Ottawa) times a week. The sampling location was at the influent of the wastewater treatment plants. Wastewater samples were collected before de-gritting in Toronto, and after for Edmonton and Ottawa.

Wastewater samples from Edmonton and Toronto were shipped to the National Microbiology Laboratory (NML) in Winnipeg, Manitoba, where SARS-CoV-2 RNA concentration was measured. RNA from wastewater samples was purified using two methods. Prior to February 12th 2021, 15 mL of clarified supernatant (after 4000 × g centrifugation for 20 min at 4°C), was concentrated using an ultracentrifugal filter device (4000 × g for 35 min at 4°C) (Amicon Ultra-15, 10 kDa MWCO, Millipore-Sigma, St. Louis, MO, U.S.A). Total RNA was extracted from the resultant concentrate (~ 200 μL) using the MagNA Pure 96 DNA and Viral NA Large Volume Kit (Roche Diagnostics, Laval, QC) using the Plasma External Lysis 4.0 protocol as per manufacturer instructions. After February 12th 2021, the pellet resultant from clarifying (4000 g for 20 min at 4°C) 30 mL of wastewater was resuspended in 700 μL Qiagen Buffer RLT (Qiagen, Germantown, MD) containing 1% 2-mercaptoethanol. To this, 200 μL of 0.5 mm zirconia-silica beads (Biospec, Bartlesville, OK) were added and the sample was processed with a Bead Mill 24 Homogenizer (Fisher Scientific, Ottawa, ON) using 4 × 30 s pulses at 6 m/s, then clarified by centrifugation (12000 × g, 3 min) and the resultant lysate used for RNA extraction using the MagNA Pure 96 instrument as described above. Viral RNA was quantified using RTq-PCR with the US-CDC N1 and N2 primers.

For Ottawa, daily 24-hour composite primary sludge samples, consisting of four discrete samples collected at 6 h intervals and subsequently mixed, were collected and transported on ice to the University of Ottawa, where samples were analyzed within 24 h of reception. Samples were concentrated by centrifugation at 10,000 g for 45 min and RNA was extracted from a 250 mg portion of the resulting pellet using a modified version of the Qiagen RNeasy PowerMicrobiome kit D'Aoust et al. (2021). Quantification was performed using singleplex probe-based RTq-PCR for the N1 and N2 gene regions of the virus.

For Edmonton and Toronto, SARS-CoV-2 RNA was extracted from the solid fraction of influent samples. The solid concentration can be affected by the influent flow volume and environmental factors such as precipitation and sedimentation Bertels et al. (2022); Amoah et al. (2022). Hence, for these locations, SARS-CoV-2 concentrations in

wastewater was normalized by the total solid suspension (TSS) measured on the sampling day at the treatment plant. For Ottawa, SARS-CoV-2 RNA concentration was normalized by the concentration of the Pepper Mild Mottle Virus (PMMoV) to account for the total human faecal mass present in the sample. Importantly, the goal of the normalization is mainly to control for the variation of other unobserved variables that can affect the viral concentration in wastewater. TSS and PMMoV may be a better proxy to control for the variations of our measured viral concentrations than daily flow because our the laboratory procedure extracts viral RNA from the solids fraction of the influent wastewater (Toronto and Edmonton) and from primary clarified sludge (Ottawa). For all cities, the reported viral concentration used in the model (W) was the average normalized concentration across all technical replicates for both the N1 and N2 genes.

We obtained clinical cases and hospital admissions (except for Toronto) for the catchment area of each of the six wastewater treatment plants. Hence, we were able to link clinical and wastewater surveillances. The data sets for the three cities are plotted in Fig. 2 Seroprevalence values at the city and province level were obtained from Canadian Blood Services (CBS) Canadian Blood Services (2021). The wastewater and clinical surveillance data used in this study are available in Supplementary File S1.

2.4.2. Fit to data

We use an Approximate Bayesian Computation (ABC) algorithm Beaumont et al. (2002) to fit the unknown or unobserved model parameters to the available data. Our observations consisted of i) SARS-CoV-2 RNA concentration in wastewater, ii) reported clinical cases of COVID-19, and iii) hospital admissions (unavailable for Toronto). For each ABC prior iteration, the error function is defined as a weighted trajectory matching

$$e_i = w_C(C - C_{\text{obs}})^2 + w_H(H - H_{\text{obs}})^2 + w_W(W - W_{\text{obs}})^2 \tag{8}$$

We use 50,000 prior ABC iterations and retain the 100 smallest errors to generate posterior distributions (acceptance ratio 2×10^{-3}). For every site, we fitted the time-dependent transmission rates (β_t), basic reproduction number (R_0), mean viral traveling time in sewer ($\bar{\tau}$) and the scaling factor for SARS-CoV-2 viral concentration measured at the sampling location (w). We chose slightly informative prior distributions to reduce the computing time (Table 2 and Appendix A-9).

The rest of the model parameters are fixed to a value based on the literature (Table 2). The parameter β_t is modelled as a piecewise linear function of time where the time partition was chosen manually to reflect the changes in trends of the reported incidence and wastewater signals. More details about the fitting procedure is given in Appendix A-1.

We define three types of fitting-to-data procedures. "Clinical" when $w_C = w_H = 1$ and $w_W = 0$, to use data from clinical sources only; "WW" when $w_W = 1$ and $w_H = w_C = 0$, to use wastewater data only; and finally "Combined" by adjusting the weights w_C, w_H and w_W such that the contribution of each of the three error terms (the squared difference in Equation 8) are, on average, approximately equal. The "Combined" fitting procedure aims to have approximately the same contribution from clinical and wastewater data sources despite the differences in observation frequencies and values (in practice, we find that w_W is about twice the value of w_C in order to reach equal contribution). The simulations are initialized with 10 infectious individuals in the compartment I_1 at the date of the first reported incidence for each location.

2.4.3. Inference of unobserved epidemiological quantities

For a given location, once the model is fitted data, we can infer unobserved quantities of epidemiological importance by generating epidemic trajectories from the posterior samples. The posterior prevalence distribution (at each time point) is defined by simply adding the populations from the compartments representing active infection, that is

$$\text{prev}(t) = E + \sum_{i=1}^{n_A} A_i + \sum_{i=1}^{n_I} I_i + \sum_{i=1}^{n_J} J_i + H \tag{9}$$

The posterior cumulative incidence is obtained by summing Equation 1a until time t

$$\text{cuminc}(t) = -\sum_{i=1}^{t} \dot{S}_i \tag{10}$$

The fitted model can also provide an estimate of the effective repro-

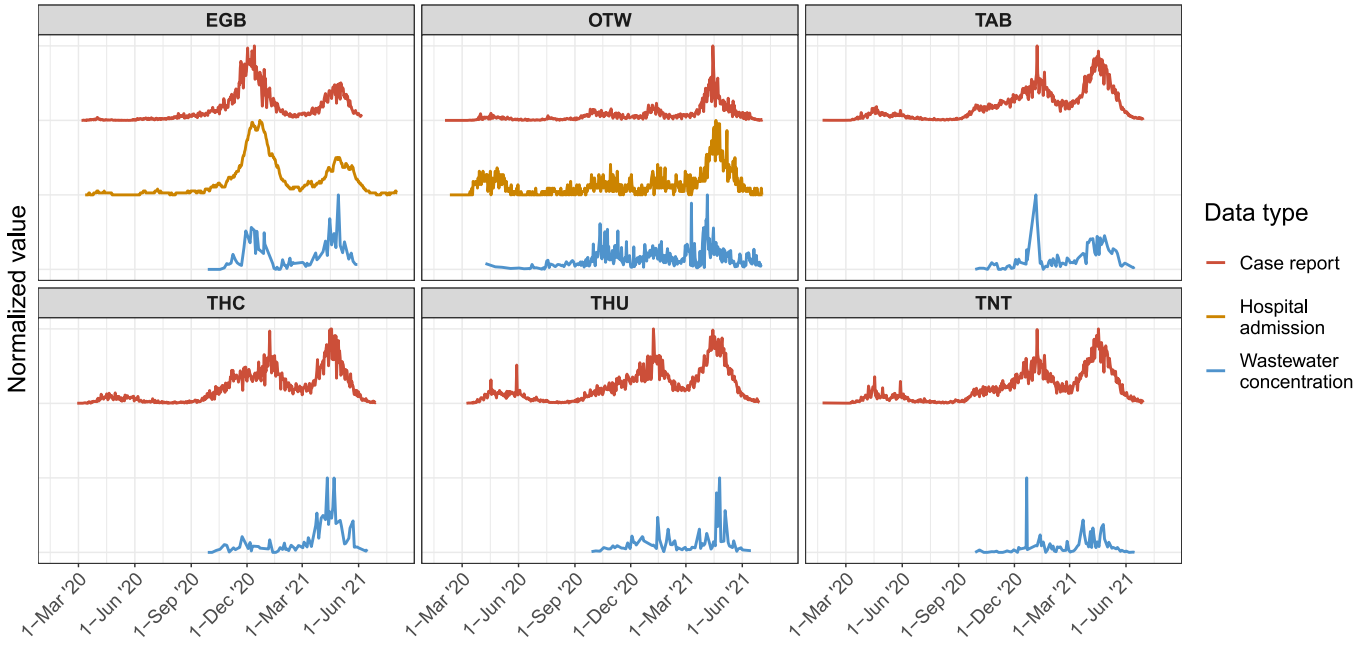

Fig. 2. Data sets used in this study for Edmonton, Ottawa and Toronto. Each horizontal panel is a city and colors represent the type of data (reported cases, hospital admissions and SARS-CoV-2 RNA concentration in wastewater). All curves were normalized to 1 (dividing by their respective maximum value) to plot them in one single panel to facilitate visual comparison. All data sets used in this study are available in Supplementary File S1.

duction number from the different data sources (e.g., clinical and/or wastewater) using Equation 2.

2.5. Simulations

2.5.1. Detection timing differential

In order to explore wastewater-based surveillance as a leading indicator of infection in the community, the time when SARS-CoV-2 is first reported from wastewater is noted d_{ww} and defined as $W(t = d_{ww}) = \text{LOD}$ where LOD is the limit of detection of the laboratory method. In addition, the time $d_{clinical}$ when COVID-19 is first reported is defined as $C(t = d_{clinical}) = 1$. Finally, we define the reported detection differential $\Delta = d_{ww} - d_{clinical}$. As a result, the wastewater signal can be classified as a leading indicator over traditional clinical surveillance when $\Delta < 0$. We assess how the reported detection differential Δ can be impacted by varying model parameters that would typically differ from one community-sewer system to another. We select only three combinations of parameters (among many) to illustrate how Δ can be affected, and most importantly how its sign can change indicating its transition between a leading and lagging indicator. We consider two levels of COVID-19 reporting, with $\rho = 30\%$ to reflect the approximate level of clinical under-reporting estimated from seroprevalence studies in Canada Canadian Blood Services (2021), and $\rho = 70\%$ that simulates a much more efficient surveillance.

2.5.2. Impact of vaccination

Although the model presented here does not explicitly have a vaccination process, we can mimic the main effects of an infection-permissive vaccine (despite high efficacy against infection, the currently available COVID-19 vaccines do not induce sterilizing immunity Focosi et al. (2022); Yewdell (2021); Reynolds et al. (2022). We model a simple scenario that rolls out an infection permissive vaccine by gradually decreasing the transmission rate (β) by 70% over 50 days and increasing the proportion of asymptomatic infection (α) from 30% to 90%. This reflects the growing protection of the population from severe outcomes of COVID-19 as well as decrease in transmissions as the vaccine is administered. To assess the differential impact of vaccination on clinical and wastewater observations, we consider the ratio of the level of SARS-CoV-2 in wastewater over the reported clinical cases, $W(t)/C(t)$.

3. Results

We present our results in two sections. First, we apply our modelling framework to wastewater and clinical surveillance data from six sampling sites located in three Canadian cities (Edmonton, Ottawa and Toronto) and infer epidemiological parameters such as prevalence, effective reproduction number and incidence forecast. The second section is based on exploratory simulations (not fitted to data of a specific location) that highlight important mechanistic aspects between clinical

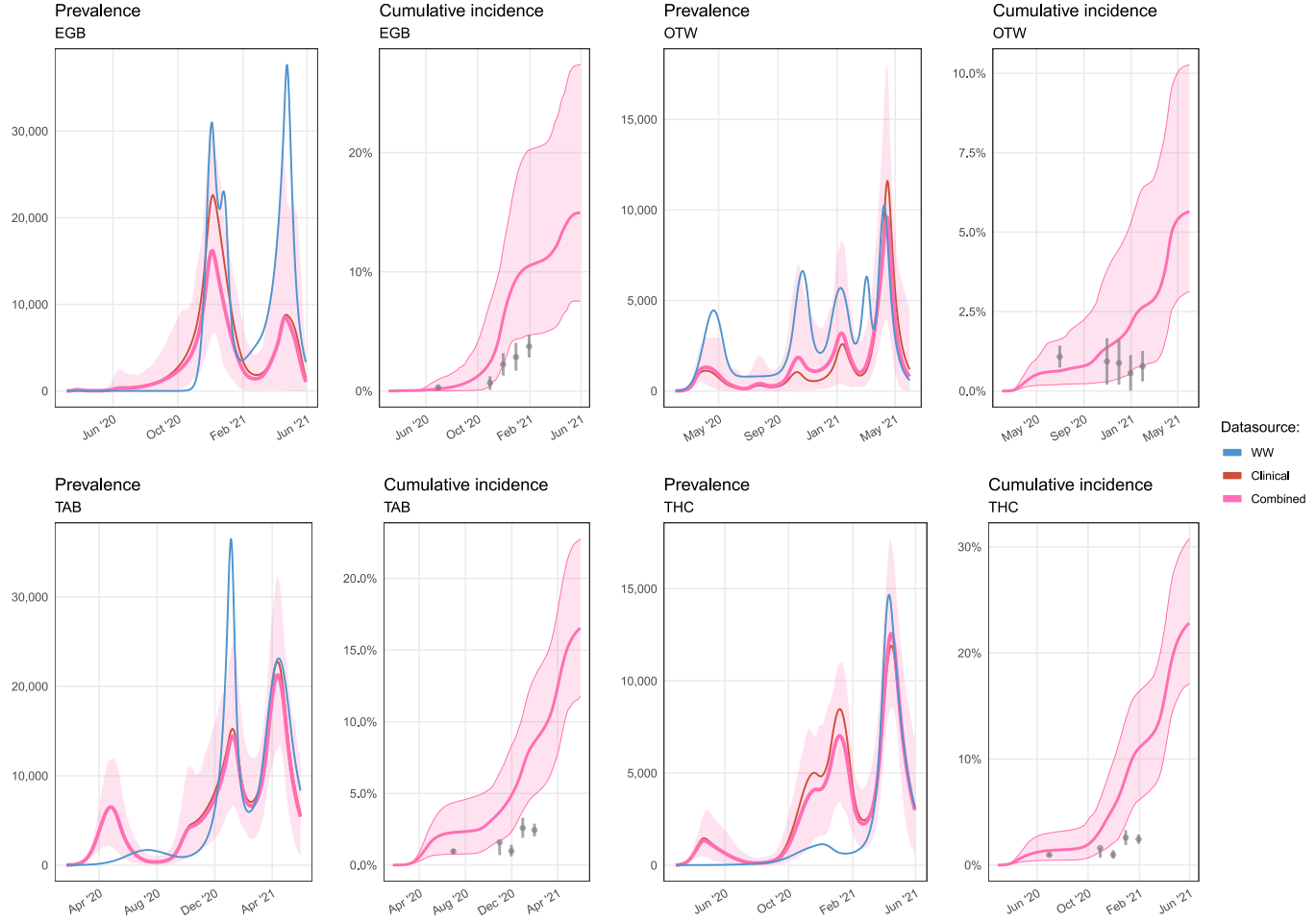

Fig. 3. SARS-CoV-2 prevalence estimates. Each quadrant block represents one of the four selected locations. The left panel of each quadrant block shows the estimates of SARS-CoV-2 prevalence in time series. The lines show the mean estimate of prevalence. The right panel of each quadrant block compares the cumulative incidence estimated by the model fitted on the "Combined" data set to seroprevalence levels reported by the Canadian Blood Services for each city (grey point indicates the mean, the vertical grey bars show the 95% confidence intervals).
(a) Each colour represents the different data sources used to fit the model (dark red: "Clinical", pink: "Combined", blue: "WW"). (b) The shaded ribbon indicates the 95% CrI for the estimate fitted on the "Combined" data set (CrIs for other data sources are shown in Appendix A-6).

and wastewater surveillances.

3.1. Application to Canadian surveillance data

In this section, we compare the inferences made on key epidemiological variables by fitting the model to different data sources. Our goal is to assess the added-value of the wastewater-based data stream. Hence, in the following, we present inferences by fitting the model to different data sources available ("Clinical", "WW" and "Combined") and comparing the outcomes. The fitting outputs from the ABC algorithm are shown in Appendix A-8 and A-9.

3.1.1. Prevalence estimates

Fig. 3 shows, for four selected locations (EGB, OTW, TAB and THC), the SARS-CoV-2 prevalence estimated by sampling the posterior distributions fitted to the various data sources "Clinical", "WW" and "Combined" and the evaluation of Equation 9. Estimates of cumulative incidence (Equation 10) from "Combined" is also displayed and compared to available SARS-CoV-2 seroprevalence levels estimated from surveys by the Canadian Blood Services performed on banks of blood donors in Edmonton, Ottawa and Toronto Canadian Blood Services (2021). Note that our model was not fitted to seroprevalence data and this comparison acts as a crude check that prevalence estimates from the model follow the same trends as other independent data sources. Cumulative incidence from wastewater data source ("WW"), compared to seroprevalence levels is also presented in Appendix A-6.

For all locations, as expected, wastewater-only prevalence estimates are close to the clinical-only ones when the levels of SARS-CoV-2 in wastewater mimic the COVID-19 trends in the population (Fig. 2). For example, the prevalence estimated from wastewater-only and clinical-only are comparable for the December 2020 wave in Edmonton and April 2021 wave in Ottawa. However, when the clinical and wastewater signals are discordant, prevalence estimates can be significantly different. For example, wastewater-based prevalence estimates in January 2021 for Toronto Highland Creek (THC) do not show the peak seen from clinical observations. On the other hand, this January peak was captured in Toronto Ashbridges Bay (TAB)–another part of the city–and the subsequent March-May 2021 wave in Toronto Highland Creek (THC) was identified by both wastewater and clinical surveillance. Further studies are needed to understand the cause(s) of the discordance observed in THC in January 2021. Finally, we note that, because of the larger variability of SARS-CoV-2 WBS and/or their lower sampling frequency as compared to daily clinical surveillance, credible intervals of our wastewater-only inferences can be larger than the clinical-only ones (see Appendix A-6).

3.1.2. Effective reproduction number

The effective reproduction number ($\mathscr{R}_t$) is a key epidemiological parameter that has gained recognition beyond public health circles during the COVID-19 pandemic Hollingsworth et al. (2020); Brauner et al. (2021). Using the same approach as for prevalence estimates, we inferred $\mathscr{R}_t$ from epidemic trajectories generated from posterior distributions fitted to the three different data sources (i.e., "Clinical", "WW" and "Combined") and Equation 2.

For comparison, we also calculate $\mathscr{R}_t$using reported COVID-19 cases using the R package EpiEstim (version 2.2) Cori et al. (2013) as a separate approach based on clinical data exclusively.

Results shown in Fig. 4 exhibit the same behaviour as for the prevalence estimates, that is, mean estimates of $\mathscr{R}_t$are similar when trends of clinical and wastewater surveillance are comparable. Despite being based on a different modelling framework, estimates from EpiEstim are consistent with clinical-only estimates from our model. Finally, like for prevalence inferences, $\mathscr{R}_t$estimates from wastewater-only data (Fig. 4, blue solid line) tend to have broader uncertainty interval compared to $\mathscr{R}_t$from clinical-only data (see Appendix A-7 for associated 95% credible interval widths).

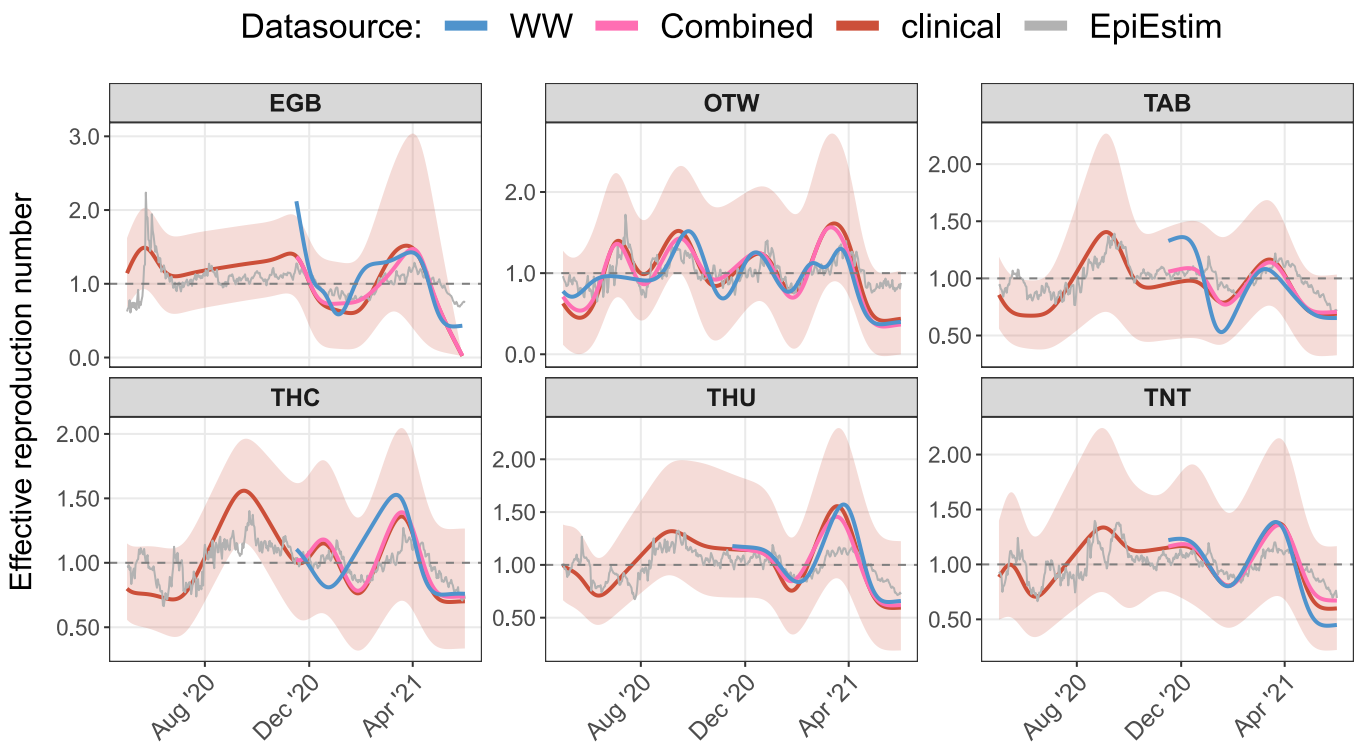

Fig. 4. Effective reproduction number. Each panel represents a wastewater treatment plant. For wastewater-based $\mathscr{R}_t$(blue curve), only estimates after 2020-Nov-15 are shown for Edmonton and Toronto to avoid the initial assay setup period. The $\mathscr{R}_t$estimates from our model are spline-smoothed, see Appendix A-7 for details. (a) Solid lines represent the mean of effective reproduction number estimated with our model for given data sources, and with the R package EpiEstim (gray). (b) The ribbon indicates the 95% credible interval for the "Clinical" data source.

3.1.3. Forecasts

Our modelling framework allows to generate forecasts based on clinical, hospital (if available) and wastewater data.

In Fig. 5 we show three 1-month-ahead forecasting examples for Edmonton, Toronto Highland Creek and Ottawa using either wastewater data only, or clinical data only. The Edmonton example (Fig. 5, left panel) shows forecasts made as of April 1st, 2021. In this case, the forecasts are relatively similar because both the clinical reports and the wastewater signals are comparable and the model fits were similar using either wastewater or clinical data. The Toronto Highland Creek example forecasts as of December 20th, 2020 (Fig. 5, middle panel). For this location, the wastewater signal and clinical reports are discordant from December 2020 to February 2021. During this period the wastewater concentration is low and approximately flat whereas the clinical reports indicate a new wave of infections. As a result, the model fitted on these two data sources interprets the epidemic differently for this period and hence provides contrasting forecasts. The forecast for Ottawa as of December 15th, 2020 (Fig. 5, right panel) illustrates the case when the wastewater forecast is more accurate than the one based on clinical surveillance only. At that time, the wastewater signal in Ottawa has picked up a resurgence earlier than clinical surveillance. This resurgence is then captured by the model fit and hence the wastewater-based forecast correctly projects the resurgence.

Here, we merely intended to demonstrate examples of successful and unsuccessful forecasts using clinical and/or wastewater data, depending on the factors influencing these estimations (including variations in testing policy, sewershed characteristics, environmental events).

3.2. Simulations

In this section, we report results from simulations that provide general insights in interpreting WBS.

3.2.1. Leading signal and reported detection differential

We vary the LOD of the wastewater assay across a broad, but realistic, range Pecson et al. (2021) and calculate Δ, the detection time difference, for each simulation for a given value of LOD and the clinical reporting rate ρ. Because SARS-CoV-2 RNA concentration in wastewater can only be determined up to a constant in our model, the LOD values chosen here are rescaled to the parameters used to run our simulations and cannot be directly interpreted as RNA copies per mL, the traditional unit for LOD. Panel A in Fig. 6 shows that, depending on the LOD of the laboratory assay, the wastewater concentration of SARS-CoV-2 RNA can either be a leading ($\Delta < 0$ for assays with low LODs) or a trailing indicator of cases (re)introduction when compared to reported clinical cases. This is the case whether the clinical surveillance system in the population is efficient or not (coloured curves, Fig. 6A).

We also vary the decay rate of RNA SARS-CoV-2 in wastewater within a broad realistic range Ahmed et al. (2020); Bivins et al. (2020); Mandal et al. (2020), as well as the transit time of SARS-CoV-2 between the shedding and sampling sites. Fig. 6B shows that, here again, the relative timing of (re)introduction detection by WBS compared to clinical surveillance can be affected by both the harshness of the wastewater (represented by the decay rate) and the transit time of SARS-CoV-2 in the sewer system. We note, as expected, that with a fast transit time (illustrated by a 1-day travel time in the left-most panel of Fig. 6) the decay rate will not have a significant impact on Δ clinical surveillance (efficient, $\rho = 70\%$, or not, $\rho = 30\%$), but as the transit time increases to 3 days (an upper bound considering strong sediment and recirculation effects) the effect of RNA decay becomes more important (increasing slope for the 1-day and 3-day transit times, Fig. 6B).

3.2.2. Decreasing trend in wastewater signal following an epidemic peak

We use a simple simulation approach to compare a declining trend of SARS-CoV-2 RNA in wastewater following a public-health measure (such as gatherings limits, compulsory face covering and lockdown) with traditional surveillance indicators such as reported cases. Previous studies Medema et al. (2020); Ahmed et al. (2020); Wurtzer et al. (2020); Peccia et al. (2020); La Rosa et al. (2020); Larsen and Wigginton (2020); Randazzo et al. (2020); D'Aoust et al. (2021); Hata et al. (2021) suggested that wastewater surveillance could confirm declining trends in clinical infections, while other studies reported an apparent decoupling Weidhaas et al. (2021). We use our mechanistic model to explore this decoupling effect with simulations.

To mimic public health interventions, we use the constant transmission rate (β) in our model and modify it to decrease linearly by 1/3 of its pre-intervention value ($\beta/3$). The time duration by which interventions can reduce the transmission rate to a steady value (time between starting date of imposed interventions and time of $\beta/3$) is captured through T_{interv}. This variable defines the speed of interventions' impact on slowing the transmission rate. For an example, a complete lockdown causing a sudden change in social contact rates and transmission rates, yet, wearing masks requires time to affect the transmission rate. We compared the relative reduction in the number of COVID-19 cases to the SARS-CoV-2 viral concentration in wastewater following 7 days of the epidemic peak by $s_{\text{cl}}(t) = C(t+7)/C(t) - 1$ and

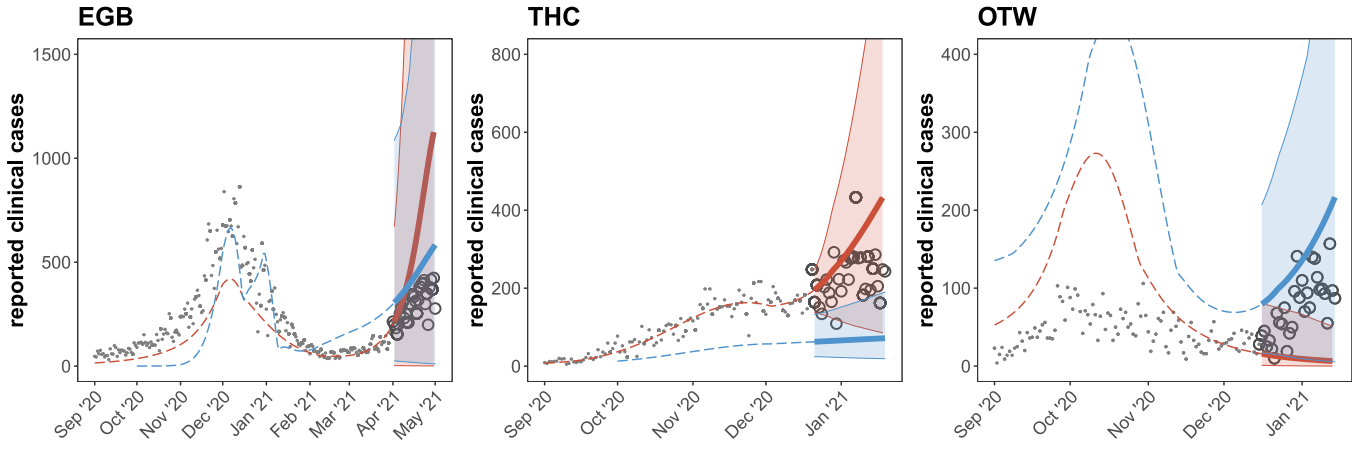

Fig. 5. Forecast examples for Edmonton (left panel), Toronto/Highland Creek (middle panel) and Ottawa (right panel). Filled points represent past data of reported clinical cases. Circles represent reported clinical cases not yet observed at the time of forecast. Colour represents the type of data the model was fitted to: blue, SARS-CoV-2 concentrations in wastewater only (past observations not shown here, for legibility); red, clinical cases only. Dashed coloured lines indicate the fitted mean for reported cases. The thick solid line shows the 1-month-ahead mean forecast, and the shaded areas their respective 95%CrI. (For interpretation of the references to colour in this figure legend, the reader is referred to the web version of this article.)

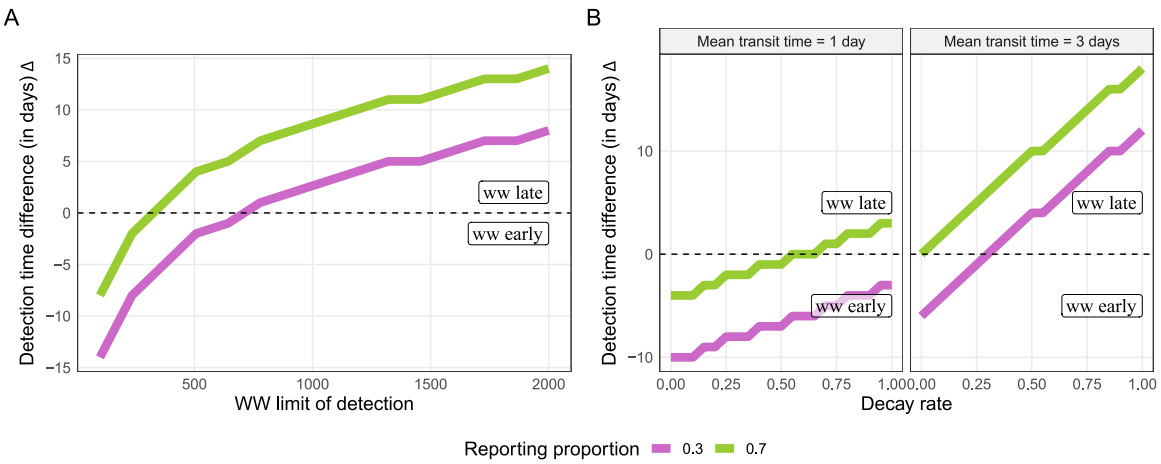

Fig. 6. Simulations were run varying selected parameters to show their impact on the reported detection time differential (Δ). Panel A: effect of the limit of detection of the quantification assay performed on wastewater. Values below the 0-intercept horizontal dashed line indicate a leading signal from wastewater concentrations than from clinical reports. Panel B: effect of the SARS-CoV-2 RNA decay rate in wastewater for different transit times between the shedding and sampling site. The colour of the curves represents the proportion of clinical cases reported (ρ) out of the total symptomatic incidence.

$s_{ww} = W(t+7)/W(t) - 1$, respectively.

Using our baseline parameters (Table 2), we simulate an intervention that reduces the contact rate to a third of its pre-intervention value at different time of the simulations, ranging from 20 to 90 days after the introduction of the index case. Fig. 7A shows that, overall, the effect of an intervention that significantly reduces transmission yields a larger relative decrease in number of COVID-19 cases than the level of SARS-CoV-2 in wastewater. The post-peak relative reduction observed in clinical surveillance (s_{cl}) is consistently larger than the one from WBS (s_{ww}) even as the timing of the intervention changes (Fig. 7B). The difference is more pronounced as the intervention reduces transmission more rapidly (T_{interv} small). Hence, given the observation noise typically encountered, we expect that the effect of a sudden change in transmission rate would be more clearly observable from clinical surveillance than from WBS. Viral concentration in wastewater tends to decline slowly following an epidemic peak and indicate an apparent decoupling with COVID-19 cases in the downward trend, caused– in our model –by the prolonged faecal shedding after infection.

3.2.3. *Differential impact of vaccination*

In Fig. 8 shows how $W(t)/C(t)$, the ratio of reported wastewater concentration over reported cases, increases following vaccination with a infection-permissive vaccine. Indeed, while an infection-permissive vaccine does reduce transmission, it still allows for infections to occur (mostly asymptomatic) and in particular, faecal shedding. Hence, a smaller proportion of infections are reported (because most of them are asymptomatic or too mild to be reported) but faecal shedding is less affected by this reporting bias and level of SARS-CoV-2 in wastewater decreases less steadily than COVID-19 surveillance. In this simulation, the approximately constant ratio before the start of vaccination (Fig. 8B) indicates that reports from clinical or wastewater data sources provide a similar picture of the epidemic for that period. However, once vaccination is implemented, the increasing ratio (Fig. 8B, green curve) highlights a discordance between the two data sources. In Appendix A-10, a short sensitivity analysis on the timing of vaccination and the duration of viral clearance shows the results presented above remain similar.

4. Discussion

Surveillance through detection and quantification of targeted pathogens in wastewater has been a noteworthy tool for public health across the world Sims and Kasprzyk-Hordern (2020); Medema et al. (2020); Wurtzer et al. (2020); Lun et al. (2018); Fioretti et al. (2018); Asghar et al. (2014); Duintjer Tebbens et al. (2017); Brouwer et al. (2018). While pathogen surveillance in wastewater is not new, the scale and urgency of scientific development for WBS are witnessed during the unprecedented COVID-19 pandemic. Because of the novelty of SARS-CoV-2-related WBS and the lack of quantitative tools for analysis, the interpretation of levels SARS-CoV-2 in wastewater and their translation into actionable public health measures is still challenging Public Health Ontario (2021b); WHO (2020); Medema et al. (2020); Foladori et al. (2020).

Here, we have provided a modelling framework to improve the understanding of the mechanisms at play between the viral transmission in the population and viral concentration shed in wastewater. This model can also provide estimates of key unobserved epidemiological parameters. We demonstrated the applicability of our model by fitting it to data from three Canadian cities and made wastewater-informed inferences of important epidemiological metrics (prevalence, effective reproduction number and forecasted incidence). Our estimates for cumulative incidence were above seroprevalence levels in all locations (Fig. 3 and Appendix A-6). Although serosurveys bring key insights on the progression of an epidemic, they may not be considered as gold-standard as their sample may not be representative of the general population. We presented their levels as an interesting comparison exercise rather than validation of the model. We also note we did not model seroreversion (patients who were infected but subsequently test seronegative because of loss of immunity or antibodies falling to undetectable levels).

Importantly, we observed that estimates based on wastewater-only data usually provide a similar picture of the epidemic trajectory (Fig. 3) but discordant signals can occur and lead to drastically different interpretations. This was the case, for example, in January 2021 in Toronto Highland Creek where the wastewater signal did not indicate a resurgence of infections, despite the wave observed from the reported clinical cases. We believe this muted peak in wastewater signal was not caused by a laboratory issue (an independent laboratory confirmed the same observation for this location), but rather from undetermined events in this particular sewershed at that specific time that need to be further investigated.

Similarly, the effective reproduction numbers inferred from wastewater data only are consistent with more traditional methods, such as using clinical reports with the software EpiEstim (Fig. 4). The fact that wastewater data can potentially act as a substitute for clinical surveillance (albeit with more uncertainty) to provide critical epidemiological metrics is encouraging, although more realistically, it will likely act as a complementary data source. The possibility to estimate epidemiological metrics using wastewater surveillance represents a step forward in

Table 2
Description of fixed and fitted parameters used in this model and their sources.

symbol	description	value/ distribution	unit	source
ξ	relative infectiousness of asymptomatic versus symptomatic	0.8	–	Landaas et al. (2021); Tian et al. (2021); Folgueira et al. (2021); Sayampanathan et al. (2021); Kociolek et al. (2020); Kissler et al. (2020)
$1/\epsilon$	latent mean duration	2	day	Li et al. (2020); He et al. (2020)
$1/\nu$	infectiousness duration for symptomatic individual	12	day	Ontario Agency for Health Protection and Promotion (Public Health Ontario) (2021); Owusu et al. (2021); Jang et al. (2021); Neant et al. (2021); Bullard et al. (2020)
$1/\mu$	infectiousness duration for symptomatic individual before admission to hospital	8	day	Murthy et al. (2021); Faes et al. (2020); He et al. (2020)
$1/\theta$	infectiousness duration for asymptomatic individual	10	day	Owusu et al. (2021); Jang et al. (2021); Neant et al. (2021); Bullard et al. (2020)
$1/\eta$	faecal shedding duration after infectious period	24	day	Hoffmann and Alsing (2021); Cuicchi et al. (2021)
$1/\ell$	length of hospital stay	11	day	Health Canada (2021); Canadian Institute for Health Information (2021)
α	asymptomatic proportion	0.316	–	Topol and Oran (2021); Mizumoto et al. (2020); Nishiura et al. (2020); Buitrago-Garcia et al. (2020)
δ	proportion of death from hospitalized	0.19	–	Canadian Institute for Health Information (2021)
ℓ_{ww}	reporting lag between sampling date and reporting date	2	day	wastewater data
κ	first-order decay rate of SARS-CoV-2 RNA in wastewater	0.18	day^{-1}	Ahmed et al. (2020); Silverman and Boehm (2020)
σ	std deviation transit time between shedding and sampling sites	0.3	day	assumed
$\overline{\tau}$	mean transit time between shedding and sampling sites	$\mathscr{U}(1,5)$	day	fitted
R_0	basic reproduction number	$\mathcal{N}(2.9,0.2)$	–	fitted
w	scaling factor for measured viral concentration at sampling location	$\mathscr{U}(0.001,0.005)$	–	fitted
h	proportion of hospital admissions per	$\mathcal{N}(0.02,,0.005)$	–	fitted
β_t	symptomatic infections time-dependent transmission rate	$\mathcal{N}$ distribution with different mean & stdev for break times in each location (see Appendix A-9)	–	fitted

attempting to use wastewater data for actionable public health metrics, if they are available to public health in a timely manner. In addition, the ability to triangulate the state of an epidemic using alternative data sources would help ensure additional confidence in the estimation of relevant parameters or forecasting. Indeed, the COVID-19 pandemic has consumed public-health resources at levels that are probably not sustainable for long-term surveillance of this pathogen. However, the current wastewater surveillance performed in many communities can probably be continued as long as necessary given its relative low cost Gawlik et al. (2021). But clearly, as our study illustrates, more research is needed to reach a level of confidence in wastewater-based surveillance that could match clinically-based surveillance.

Our modelling framework provides a more principled alternative to simpler smoothing techniques (e.g., moving averages, polynomial interpolations) that have been used to support the interpretation of WBS D'Aoust et al. (2021). However, we note that less complex modelling options are possible if the focus is on specific epidemiological metrics (Huisman et al. (2021); Xiao et al. (2021)). We also note recent efforts to use machine learning techniques and artificial neural network that incorporate WBS Li et al. (2021). While those methods are promising, they cannot–by design–explain the epidemiological mechanisms at play.

Our model enables *in silico* experiments on the epidemic/wastewater system to identify key parameters and processes that can play an important role for the epidemiological interpretation. We showed, using simulations, that the relative timing of the wastewater signal (whether it is leading or not) compared to traditional clinical surveillance is actually influenced by the characteristics of *both* systems (Fig. 6). On the one hand, the laboratory analysis of wastewater samples may not detect the presence of SARS-CoV-2 because, for example, its limit of detection is too high, or prevalence of infection in the community is very small, or the viral RNA has degraded before reaching the sampling site. Shipment time of wastewater samples can also be significant (e.g., several days) for remote sampling locations without any laboratory capacity. On the other hand, the delay in clinical cases reports is usually caused by the incubation period and the reporting time of an infection by the health system (turnaround time for contact tracing and/or laboratory results of individuals' swab) or availability of testing. Some communities would typically have a longer lag for clinical reporting than for wastewater surveillance La Rosa et al. (2020); Randazzo et al. (2020); D'Aoust et al. (2021); Hata et al. (2021), while others may have the opposite (for example when a very effective contact tracing system is in place Mettler et al. (2020) or rapid testing is implemented). Moreover, a community may experience both situations, that is a period when clinical surveillance is extremely efficient at detecting cases so rapidly that it leads wastewater surveillance while, at other times, it can lag (for example when incidence is high, overwhelming contact-tracing and clinical testing capacities). The model presented here allows to quantify how various factors can impacts the relative timing between clinical and wastewater surveillances.

It can be tempting to monitor the effect of public health interventions using changes in the levels of SARS-CoV-2 in wastewater given its non-invasive nature. Indeed, WBS should be less affected by sampling bias than clinical surveillance (for example the latter may miss most of the

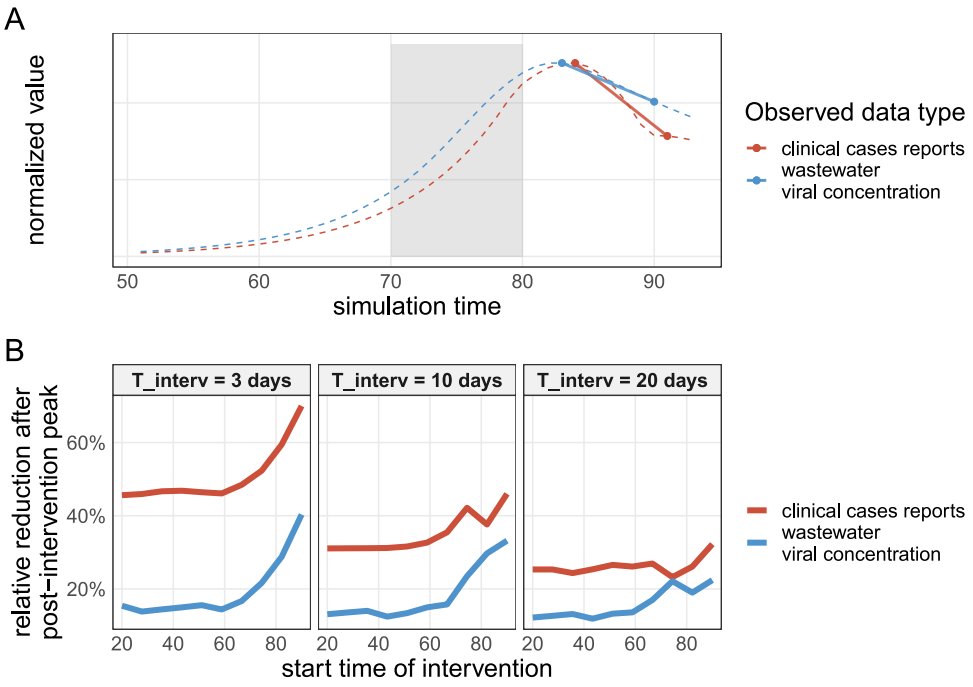

Fig. 7. Detectability of a sharp transmission reduction. Panel A: example of how the post-peak relative changes are calculated. The colour-coded dashed lines represent the time series of reported clinical cases and SARS-CoV-2 RNA concentration in wastewater. The grey shaded area indicates when the transmission rate decreases (here, $T_{\text{interv}} = 10$ days). The segment illustrates the relative change between the peak value and 7 days later (s_{ww} and s_{cl}),i.e., how we would typically assess the efficacy to reduce transmission. Panel B: the horizontal axis represents the time (since the start of the epidemic) when transmission begins to reduce to a third of its value. The vertical axis represents the post-peak relative changes from clinical reports (s_{cl}, red lines) or wastewater (s_{ww}, blue lines). Each subpanel indicates a different value (3, 10 and 20 days) for T_{interv}, the time it takes to reduces the transmission rate to a third of its initial value. (For interpretation of the references to colour in this figure legend, the reader is referred to the web version of this article.)

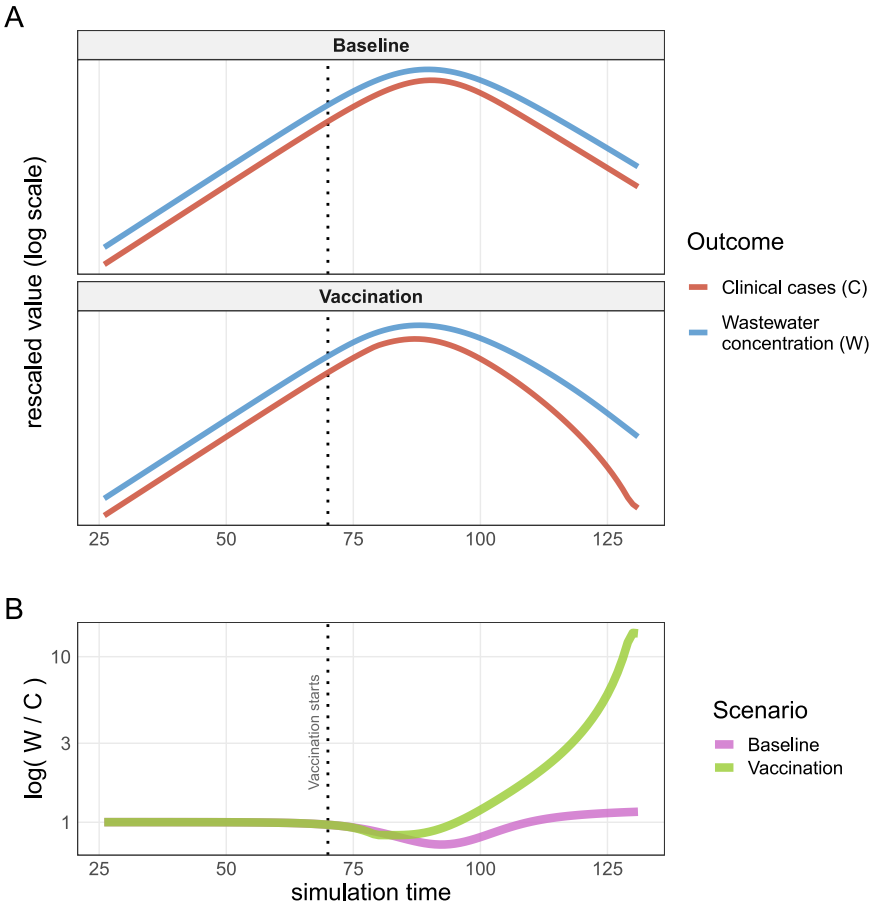

Fig. 8. Infection-permissive vaccination. Panel A shows the trajectories of reported clinical cases and SARS-CoV-2 concentration in wastewater under a scenario using an infection-permissive vaccine ("Vaccination"), or not ("Baseline"). In the vaccination scenario, the reported clinical cases decrease more rapidly than the level of SARS-CoV-2 in wastewater because sub-clinical infections tend to be less reported whereas faecal shedding continues. Panel B highlights this difference showing $W(t)/C(t)$, the ratio of reported wastewater concentration over reported cases, for the baseline / no-vaccination (pink) and the vaccination (green) scenarios. The ratio is normalized to have a starting value at 1 to make it easier to quantify the increase visually. The vertical dotted line indicates when vaccination starts (at time 70). (For interpretation of the references to colour in this figure legend, the reader is referred to the web version of this article.)

subclinical infections). However, our simulations showed that wastewater surveillance may be inferior to clinical surveillance to identify sharp declines in transmission, as typically seen after a lockdown is implemented (Fig. 7). The long period of faecal shedding creates a lag in comparison to the sudden drop of incidence caused by the public health intervention, inhibiting a prompt signal in wastewater. This effect is visible on the Canadian data sets presented here (Fig. 2). We note that this result may not be valid for laboratory assay with a high limit of

detection of SARS-CoV-2 RNA in wastewater.We also highlight the potential for an infection-permissive vaccine to generate discordant signals between wastewater and clinical surveillances (Fig. 8). Indeed, vaccination implies a larger proportion of asymptomatic infections which are less likely to be detected by clinical surveillance, but still picked up in wastewater because of continued faecal shedding. Note that we use our model to highlight this potential effect, whereas detecting it in real data is probably challenging without studies purposely designed to detect this.

Here, we used a mixed approach regarding the normalization of the levels of SARS-CoV-2 in wastewater, with Ottawa using PMMoV-normalization versus TSS-normalization for Toronto and Edmonton. It is likely that some normalization is necessary to discount the in-sewer daily fluctuations resulting from environmental factors (PH, ammonia, temperature, precipitation, etc.), sampling methods and total mass of faecal shedded, but it is still not clear which normalization is the most appropriate for a given sewershed and the type of sampled wastewater (influent liquid versus solid). A recent study Kim et al. (2022) showed that SARS-CoV-2 concentration measurements from solid samples with PMMoV normalization produce comparable results between different laboratory methods and across sampling locations but comparability was not observed for viral measurements from liquid influent wastewater, perhaps due to multiple recovery methods for liquid wastewater which each extracts different recovered fractions of the SARS-CoV-2 RNA concentration at different efficiencies. This might explain the reduced correlation between COVID-19 case counts and SARS-CoV-2 N1/N2 genes in influent wastewater samples which are normalized with human faecal markers (e.g., PMMoV) Feng et al. (2021). Hence, the choice of normalization might be more relevant to the type of wastewater sample analyzed (liquid versus solid fraction).

Our modelling approach has several weaknesses. Forecasts and $\mathscr{R}_t$ estimations depend on the quality of the model fitting to data and here, we used a simple ABC algorithm that could certainly be improved. However, the model reasonably fit to data for most locations (Appendix A-8 and A-9). In general, fitting the model to the combined clinical and wastewater surveillance ("Combined") might not be the best practice in the long run because of the reduction of traditional surveillance to pre-pandemic levels. Given the multiple sources of uncertainties associated with the wastewater data, we think that informing the model with combined data sets may provide a better triangulation of the pandemic.

We did not precisely model the transport and fate of SARS-CoV-2 in municipal sewer systems. The lack of data about flow dynamics and particles binding of SARS-CoV-2 in wastewater hampered a more detailed approach. Hence, we took a simple approach to model the below-ground component and assumed the flow dynamic followed a low-dispersion plug flow model with a plausible fixed decay rate Ahmed et al. (2020) and let vary the mean transit time (from shedding to sampling sites) within a range of possible values. As more research focuses on the fate of SARS-CoV-2 in wastewater, the transport module of our model can be enhanced.Our model does not model vaccination explicitly. We made this choice to keep the first version of our model relatively simple. However, we believe that we can appropriately approximate the effects of infection-permissive vaccination by reducing the transmission rate and increasing the proportion of asymptomatic infections. As the proportion of vaccinated individuals increases, modelling an explicit vaccination process is necessary. We note that for the Canadian cities studied here, the vaccination coverage was either null or low during the study period. We model SARS-CoV-2 as a single-strain pathogen which is an oversimplification of reality, given the numerous variants circulating in Canada since late 2020 McLaughlin et al. (2021). However, it is not clear how (or if) multi-variants modelling would affect our results, given that the difference of viral shedding (respiratory and faecal) between variants is still not fully understood Kidd et al. (2021); Kissler et al. (2021). Because of ordinary differential equations, this model is not well adapted to either small communities or very low prevalence settings. While its epidemiological structure (Fig. 1) would still be valid for such environments, a more advanced statistical modelling would be preferable to handle low incidence counts and observation uncertainty King et al. (2015); Li et al. (2018). A further limitation of our model is the use of a scaling coefficient for the amount of SARS-CoV-2 shedded in the wastewater by the infected population (parameter ω in Equation 3). This scaling coefficient embeds all the uncertainties associated with sampling strategy and laboratory analysis, such as assay recovery efficiency, limit of detection, and total faecal mass normalization. Most of those processes are currently poorly known for SARS-CoV-2 and, as long as more observational data is not available, will constrain modelling (note that this limitation has already been identified for polio models Brouwer et al. (2018)). An ultimate goal of wastewater surveillance may be to measure all the components of the scaling coefficient (here, ω) in order to estimate infection prevalence in a community directly from viral concentration readings.

To conclude, the model presented here–built upon previous similar approach for other pathogens McMahan et al. (2020); Brouwer et al. (2018); Kraay et al. (2018)–is a first step to better understand the mechanistic relationships between the COVID-19 epidemic spreading in a community and the SARS-CoV-2 RNA concentration in wastewater caused by faecal shedding of infected individuals (and potentially from urinary or sputum shedding). Future developments should explicitly incorporate vaccination and multiple variants/strains given the ability of new assays to detect variants from wastewater samples La Rosa et al. (2021); Agrawal et al. (2021); Jahn et al. (2021). This model can be the basis of quantitative tools to support public health decision making that embraces wastewater-based epidemiology. Beyond the SARS-CoV-2/COVID-19 pandemic, WBS coupled with the type of model presented here could be leveraged and applied to other transmissible pathogens where urinary or faecal shedding occurs, such as other respiratory diseases (e.g., influenza, respiratory syncytial virus, adenovirus) and some enteric diseases (e.g., norovirus, rotavirus, shigellosis).

Funding

Robert Delatolla acknowledges funding by Ontario Ministry of Environment Conservation and Parks Wastewater Surveillance Initiative Transfer Payment Agreement 2020–11–1–1463261970.

Declaration of Competing Interest

All authors declare they do not have any competing interests.

Acknowledgments

Wastewater samples from Edmonton and Toronto were provided to the NML through a collaboration with Statistics Canada's Canadian Wastewater Survey. Dave Spreitzer, Ravinder Lidder, Codey Dueck, Quinn Wonitowy, Umar Mohammed and Graham Cox for their contribution in wastewater sample processing and technical assistance. Dana Al-Bargash provided data and local expertise for the City of Toronto. The wastewater treatment plant Gold Bar, EPCOR Water Services Inc., Edmonton, Alberta, Canada for providing sewage samples in this study for the city of Edmonton. Peter Vanrolleghen's group at the Université Laval (QC, Canada) for insightful discussions on viral transport and fate in wastewater.

Appendix A. Supporting information

Supplementary data associated with this article can be found in the online version at doi:10.1016/j.epidem.2022.100560.

References

Agrawal, S., Orschler, L., Schubert, S., Zachmann, K., Heijnen, L., Tavazzi, S., Gawlik, B. M., de Graaf, M., Medema, G., Lackner, S., 2021. A pan-European study of SARS-CoV-2 variants in wastewater under the EU Sewage Sentinel System (Jun). medRxiv (Jun).

Ahmed, W., Angel, N., Edson, J., Bibby, K., Bivins, A., O'Brien, J.W., Choi, P.M., Kitajima, M., Simpson, S.L., Li, J., Tscharke, B., Verhagen, R., Smith, W.J.M., Zaugg, J., Dierens, L., Hugenholtz, P., Thomas, K.V., Mueller, J.F., 2020. First confirmed detection of SARS-CoV-2 in untreated wastewater in Australia: a proof of concept for the wastewater surveillance of COVID-19 in the community (Aug). Sci. Total Environ. 728, 138764 (Aug).

Ahmed, Warish, Bertsch, Paul M., Bibby, Kyle, Haramoto, Eiji, Hewitt, Joanne, Huygens, Flavia, Gyawali, Pradip, Korajkic, Asja, Riddell, Shane, Sherchan, Samendra P., Simpson, Stuart L., Sirikanchana, Kwanrawee, Symonds, Erin M., Verhagen, Rory, Vasan, Seshadri S., Kitajima, Masaaki, Bivins, Aaron, 2020. Decay of sars-cov-2 and surrogate murine hepatitis virus rna in untreated wastewater to inform application in wastewater-based epidemiology. Environ. Res. 191, 110092.

Amoah, I.D., Abunama, T., Awolusi, O.O., Pillay, L., Pillay, K., Kumari, S., Bux, F., 2022. Effect of selected wastewater characteristics on estimation of SARS-CoV-2 viral load in wastewater. Environ. Res. 203 (111877), 01.

Anderson, Roy M., May, Robert M., 1991. Infectious Diseases of Humans. Dynamics and Control. Oxford University Press.

Asghar, H., Diop, O.M., Weldegebriel, G., Malik, F., Shetty, S., ElBassioni, L., Akande, A. O., AlMaamoun, E., Zaidi, S., Adeniji, A.J., Burns, C.C., Deshpande, J., Oberste, M.S., Lowther, S.A., 2014. Environmental surveillance for polioviruses in the global polio eradication initiative (Nov). J. Infect Dis. 210 (Suppl 1), 294–303 (Nov).

Beaumont, MarkA, Zhang, Wenyang, Balding, David J., 2002. Approximate bayesian computation in population genetics, 12 Genetics 162 (4), 2025–2035, 12.

Bertels, X., Demeyer, P., Van den Bogaert, S., Boogaerts, T., van Nuijs, A.L.N., Delputte, P., Lahousse, L., 2022. Factors influencing SARS-CoV-2 RNA concentrations in wastewater up to the sampling stage: a systematic review (Jan). Sci. Total Environ., 153290 (Jan).

Bivins, Aaron, Greaves, Justin, Fischer, Robert, Yinda, KweClaude, Ahmed, Warish, Kitajima, Masaaki, Munster, Vincent J., Bibby, Kyle, 2020. Persistence of sars-cov-2 in water and wastewater. Environ. Sci. Technol. Lett. 7 (12), 937–942.

Brauner, J.M., Mindermann, S., Sharma, M., Johnston, D., Salvatier, J., Gaven?iak, T., Stephenson, A.B., Leech, G., Altman, G., Mikulik, V., Norman, A.J., Monrad, J.T., Besiroglu, T., Ge, H., Hartwick, M.A., Teh, Y.W., Chindelevitch, L., Gal, Y., Kulveit, J., 2021. ScienceInferring the effectiveness of government interventions against COVID-19. Science 371 (6531), 02.

Brouwer, Andrew F., Eisenberg, Joseph N.S., Pomeroy, Connor D., Shulman, Lester M., Hindiyeh, Musa, Manor, Yossi, Grotto, Itamar, Koopman, James S., Eisenberg, Marisa C., 2018. Epidemiology of the silent polio outbreak in rahat, israel, based on modeling of environmental surveillance data. Proceedings of the National Academy of Sciences 115 (45), E10625–E10633.

Buitrago-Garcia, D., Egli-Gany, D., Counotte, M.J., Hossmann, S., Imeri, H., Ipekci, A.M., Salanti, G., Low, N., 2020. Occurrence and transmission potential of asymptomatic and presymptomatic SARS-CoV-2 infections: a living systematic review and meta-analysis, 09 PLoS Med. 17 (9), e1003346, 09.

Bullard, Jared, Dust, Kerry, Funk, Duane, Strong, James E., Alexander, David, Garnett, Lauren, Boodman, Carl, Bello, Alexander, Hedley, Adam, Schiffman, Zachary, Doan, Kaylie, Bastien, Nathalie, Li, Yan, Van Caeseele, Paul G., Poliquin, Guillaume, 2020. Predicting infectious severe acute respiratory syndrome coronavirus 2 from diagnostic samples, 05 Clin. Infect. Dis. 71 (10), 2663–2666, 05.

Canadian Blood Services.Covid-19 public seroprevalence report: April 2020 to january 2021. Technical report, Canadian Blood Services, 2021.

Canadian Institute for Health Information.Covid-19 hospitalization and emergency department statistics, 2019–2020 and 2020–2021. Ottawa, ON: CIHI, 03 2021.

Christou, A., Aguera, A., Bayona, J.M., Cytryn, E., Fotopoulos, V., Lambropoulou, D., Manaia, C.M., Michael, C., Revitt, M., Schröder, P., Fatta-Kassinos, D., 2017. The potential implications of reclaimed wastewater reuse for irrigation on the agricultural environment: the knowns and unknowns of the fate of antibiotics and antibiotic resistant bacteria and resistance genes - A review. Water Res. 123 (448–467), 10.

City of Ottawa.Wastewater collection and treatment, Robert O. Pickard Environmental Centre (ROPEC). Online, 2021.

Cori, A., Ferguson, N.M., Fraser, C., Cauchemez, S., 2013. A new framework and software to estimate time-varying reproduction numbers during epidemics (October). Am. J. Epidemiol. 178 (9), 1505–1512 (October).

Cuicchi, D., Lazzarotto, T., Poggioli, G., 2021. Fecal-oral transmission of SARS-CoV-2: review of laboratory-confirmed virus in gastrointestinal system (Mar). Int. J. Colorectal Dis. 36 (3), 437–444 (Mar).

D'Aoust, P.M., Graber, T.E., Mercier, E., Montpetit, D., Alexandrov, I., Neault, N., Baig, A.T., Mayne, J., Zhang, X., Alain, T., Servos, M.R., Srikanthan, N., MacKenzie, M., Figeys, D., Manuel, D., Juni, P., MacKenzie, A.E., Delatolla, R., 2021 (May). Catching a resurgence: Increase in SARS-CoV-2 viral RNA identified in wastewater 48h before COVID-19 clinical tests and 96h before hospitalizations 770, 145319 (May).

D'Aoust, P.M., Mercier, E., Montpetit, D., Jia, J.J., Alexandrov, I., Neault, N., Baig, A.T., Mayne, J., Zhang, X., Alain, T., Langlois, M.A., Servos, M.R., MacKenzie, M., Figeys, D., MacKenzie, A.E., Graber, T.E., Delatolla, R., 2021. Quantitative analysis of SARS-CoV-2 RNA from wastewater solids in communities with low COVID-19 incidence and prevalence (Jan). Water Res. 188, 116560 (Jan).

DuintjerTebbens, R.J., Zimmermann, M., Pallansch, M.A., Thompson, K.M., 2017. Insights from a systematic search for information on designs, costs, and effectiveness of poliovirus environmental surveillance systems, 12 Food Environ. Virol. 9 (4), 361–382, 12.

Faes, C., Abrams, S., Van Beckhoven, D., Meyfroidt, G., Vlieghe, E., Hens, N., Aouachria, A.S., Bafort, K., Belkhir, L., Bossuyt, N., Colombie, V., Dauby, N., De Munter, P., Deblonde, J., Delmarcelle, D., Delvallee, M., Demeester, R., Dugernier, T., Holemans, X., Kerzmann, B., Machurot, P.Y., Minette, P., Minon, J.M., Mokrane, S., Nachtergal, C., Noirhomme, S., Pierard, D., Rossi, C., Schirvel, C., Sermijn, E., Staelens, F., Triest, F., Van Goethem, N., Van Praet, J., Vanhoenacker, A., Cooreman, S., Willems, E., Wyndham-Thomas, C., 2020. Time between symptom onset, hospitalisation and recovery or death: statistical analysis of Belgian COVID-19 patients. Int. J. Environ. Res. Public Health 17 (20), 10.

Feng, Lizhou, Zhang, Wei, Li, Xiqing, 2018. Monitoring of regional drug abuse through wastewater-based epidemiology? A critical review(article). Sci. China Earth Sci. 61 (3), 239–255.

Feng, Shuchen, Roguet, Adelaide, McClary-Gutierrez, Jill S., Newton, Ryan J., Kloczko, Nathan, Meiman, JoNathan G., McLellan, Sandra L., 2021. Evaluation of sampling, analysis, and normalization methods for sars-cov-2 concentrations in wastewater to assess covid-19 burdens in wisconsin communities. ACS ES&T Water 1 (8), 1955–1965.

Fioretti, J.M., Fumian, T.M., Rocha, M.S., DosSantos, I.A.L., Carvalho-Costa, F.A., de Assis, M.R., Rodrigues, J.S., Leite, J.P.G., Miagostovich, M.P., 2018. Surveillance of Noroviruses in Rio De Janeiro, Brazil: occurrence of New GIV genotype in clinical and wastewater samples, 03 Food Environ. Virol. 10 (1), 1–6, 03.

Daniele Focosi, Fabrizio Maggi, and Arturo Casadevall.Mucosal vaccines, sterilizing immunity, and the future of sars-cov-2 virulence. Viruses, 14(2), February 2022. Publisher Copyright: © 2022 by the authors. Licensee MDPI, Basel, Switzerland.

Foladori, Paola, Cutrupi, Francesca, Segata, Nicola, Manara, Serena, Pinto, Federica, Malpei, Francesca, Bruni, Laura, Rosa, GiuseppinaLa, 2020. Sars-cov-2 from faeces to wastewater treatment: what do we know? a review. Sci. Total Environ. 743, 140444.

Folgueira, M.D., Luczkowiak, J., Lasala, F., Perez-Rivilla, A., Delgado, R., 2021. Prolonged SARS-CoV-2 cell culture replication in respiratory samples from patients with severe COVID-19 (Feb). Clin. Microbiol. Infect. (Feb).

BM Gawlik, i S. Tavazz, G. Mariani, H. Skejo, M. Sponar, T. Higgins, G. Medema, and T. Wintgens.Sars-cov-2 surveillance employing sewage. towards a sentinel system. Technical report, European Union, 2021.

Gibas, C., Lambirth, K., Mittal, N., Juel, M.A.I., Barua, V.B., Roppolo Brazell, L., Hinton, K., Lontai, J., Stark, N., Young, I., Quach, C., Russ, M., Kauer, J., Nicolosi, B., Chen, D., Akella, S., Tang, W., Schlueter, J., Munir, M., 2021. Implementing building-level SARS-CoV-2 wastewater surveillance on a university campus (Aug). Sci. Total Environ. 782, 146749 (Aug).

Gundy, P.M., Gerba, C.P., Pepper, I.L., 2009. Survival of coronaviruses in water and wastewater. Food Environ. Virol.

Hata, A., Hara-Yamamura, H., Meuchi, Y., Imai, S., Honda, R., 2021. Detection of SARS-CoV-2 in wastewater in Japan during a COVID-19 outbreak (Mar). Sci. Total Environ. 758, 143578 (Mar).

He, X., Lau, E.H.Y., Wu, P., Deng, X., Wang, J., Hao, X., Lau, Y.C., Wong, J.Y., Guan, Y., Tan, X., Mo, X., Chen, Y., Liao, B., Chen, W., Hu, F., Zhang, Q., Zhong, M., Wu, Y., Zhao, L., Zhang, F., Cowling, B.J., Li, F., Leung, G.M., 2020. Temporal dynamics in viral shedding and transmissibility of COVID-19, 05 Nat Med. 26 (5), 672–675, 05.

Health Canada.Covid-19 discharge abstract database metadata (dad).2021.

Hoffmann, Till, Alsing, Justin, 2021. Faecal shedding models for sars-cov-2rna amongst hospitalised patients and implications for wastewater-based epidemiology. medRxiv.

Hollingsworth, C., Keeling, D., Vegvari, M., Baggaley, C., Maddren, R., Anderson, R., Donnelly, R., 2020. Reproduction number (R) and growth rate (r) of the COVID-19 epidemic in the UK: methods of estimation, data sources, causes of heterogeneity, and use as a guide in policy formulation. The Royal Soc.

Huisman, Jana S., Scire, Jérémie, Caduff, Lea, Fernandez-Cassi, Xavier, Ganesanandamoorthy, Pravin, Kull, Anina, Scheidegger, Andreas, Stachler, Elyse, Boehm, Alexandria B., Hughes, Bridgette, Knudson, Alisha, Topol, Aaron, Wigginton, Krista R., Wolfe, Marlene K., Kohn, Tamar, Ort, Christoph, Stadler, Tanja, Julian, Timothy R., 2021. Wastewater-based estimation of the effective reproductive number of sars-cov-2. medRxiv.

Jahn, Katharina, Dreifuss, David, Topolsky, Ivan, Kull, Anina, Ganesanandamoorthy, Pravin, Fernandez-Cassi, Xavier, Bänziger, Carola, Stachler, Elyse, Fuhrmann, Lara, Jablonski, Kim Philipp, Chen, Chaoran, Aquino, Catharine, Stadler, Tanja, Ort, Christoph, Kohn, Tamar, Julian, Timothy R., Beerenwinkel, Niko, 2021. Detection of sars-cov-2 variants in switzerland by genomic analysis of wastewater samples. medRxiv.

Jang, Sukbin, Rhee, Ji-Young, Wi, Yu Mi, Jung, Bo Kyeung, 2021. Viral kinetics of sars-cov-2 over the preclinical, clinical, and postclinical period. Intern. J. Infect. Dis. 102, 561–565.

Jones, David L., Quintela Baluja, Marcos, Graham, David W., Corbishley, Alexander, McDonald, James E., Malham, Shelagh K., Hillary, Luke S., Connor, Thomas R., Gaze, William H., Moura, Ines B., Wilcox, Mark H., Farkas, Kata, 2020. Shedding of sars-cov-2 in feces and urine and its potential role in person-to-person transmission and the environment-based spread of covid-19. Sci. Total Environ. 749, 141364.

Kayode Coker, A., 2001. Chapter eight - residence time distributions in flow reactors 663–761.

Kidd, Michael, Richter, Alex, Best, Angus, Cumley, Nicola, Mirza, Jeremy, Percival, Benita, Mayhew, Megan, Megram, Oliver, Ashford, Fiona, White, Thomas, Moles-Garcia, Emma, Crawford, Liam, Bosworth, Andrew, Atabani, Sowsan F., Plant, Tim, McNally, Alan, 2021. S-Variant SARS-CoV-2 Lineage B1.1.7 Is associated with significantly higher viral load in samples tested by taqpath polymerase chain reaction, 02 J. Infect. Dis. 223 (10), 1666–1670, 02.

Kim, Sooyeol, Kennedy, Lauren C., Wolfe, Marlene K., Criddle, Craig S., Duong, Dorothea H., Topol, Aaron, White, Bradley J., Kantor, Rose S., Nelson, Kara L., Steele, Joshua A., Langlois, Kylie, Griffith, John F., Zimmer-Faust, Amity G., McLellan, Sandra L., Schussman, Melissa K., Ammerman, Michelle, Wigginton, Krista R., Bakker, Kevin M., Boehm, Alexandria B., 2022. Sars-cov-2 rna is enriched by orders of magnitude in primary settled solids relative to liquid wastewater at publicly owned treatment works (pages -). Environ. Sci.: Water Res. Technol. (pages -).

King, A.A., Domenech de Celles, M., Magpantay, FM G., Rohani, P., 2015. Avoidable errors in the modelling of outbreaks of emerging pathogens, 20150347-20150347, April with special reference to Ebola. Proceedings of the Royal Society B: Biological Sciences 282 (1806), 20150347-20150347, April.

Kissler, Stephen M., Fauver, Joseph R., Mack, Christina, Olesen, Scott W., Tai, Caroline, Shiue, Kristin Y., Kalinich, Chaney C., Jednak, Sarah, Ott, Isabel M., Vogels, Chantal B.F., Wohlgemuth, Jay, Weisberger, James, DiFiori, John, Anderson, Deverick J., Mancell, Jimmie, Ho, David D., Grubaugh, Nathan D., Grad, Yonatan H., 2020. Sars-cov-2 viral dynamics in acute infections. medRxiv.

Kissler, Stephen M., Fauver, Joseph R., Mack, Christina, Tai, Caroline G., Breban, Mallery I., Watkins, Anne E., Samant, Radhika M., Anderson, Deverick J., Ho, David D., Metti, Jessica, Khullar, Gaurav, Baits, Rachel, MacKay, Matthew, Salgado, Daisy, Baker, Tim, Dudley, Joel T., Mason, Christopher E., Grubaugh, Nathan D., Grad, Yonatan H., 2021. Densely sampled viral trajectories for sars-cov-2 variants alpha (b.1.1.7) and epsilon (b.1.429). medRxiv.

Kitajima, M., Ahmed, W., Bibby, K., Carducci, A., Gerba, C.P., Hamilton, K.A., Haramoto, E., Rose, J.B., 2020 (Oct). SARS-CoV-2 in wastewater: State of the knowledge and research needs 739, 139076 (Oct).

Kociolek, L.K., Muller, W.J., Yee, R., DienBard, J., Brown, C.A., Revell, P.A., Wardell, H., Savage, T.J., Jung, S., Dominguez, S., Parikh, B.A., Jerris, R.C., Kehl, S.C., Campigotto, A., Bender, J.M., Zheng, X., Muscat, E., Linam, M., Abuogi, L., Smith, C., Graff, K., Hernandez-Leyva, A., Williams, D., Pollock, N.R., 2020. Comparison of upper respiratory viral load distributions in asymptomatic and symptomatic children diagnosed with SARS-CoV-2 infection in pediatric hospital testing programs. J. Clin. Microbiol. 59 (1), 12.

Kraay, A.N.M., Brouwer, A.F., Lin, N., Collender, P.A., Remais, J.V., Eisenberg, J.N.S., 2018. Proc Natl Acad Sci U S AModeling environmentally mediated rotavirus transmission: The role of temperature and hydrologic factors, 03 Proc. Natl. Acad. Sci. U.S.A 115 (12), E2782–E2790, 03.

La Rosa, G., Iaconelli, M., Mancini, P., Bonanno Ferraro, G., Veneri, C., Bonadonna, L., Lucentini, L., Suffredini, E., 2020. First detection of SARS-CoV-2 in untreated wastewaters in Italy (Sep). Sci. Total Environ. 736, 139652 (Sep).

La Rosa, G., Mancini, P., BonannoFerraro, G., Veneri, C., Iaconelli, M., Lucentini, L., Bonadonna, L., Brusaferro, S., Brandtner, D., Fasanella, A., Pace, L., Parisi, A., Galante, D., Suffredini, E., 2021 (Jun). Rapid screening for SARS-CoV-2 variants of concern in clinical and environmental samples using nested RT-PCR assays targeting key mutations of the spike protein 197, 117104 (Jun).

Laht, M., Karkman, A., Voolaid, V., Ritz, C., Tenson, T., Virta, M., Kisand, V., 2014. Abundances of tetracycline, sulphonamide and beta-lactam antibiotic resistance genes in conventional wastewater treatment plants (WWTPs) with different waste load. PLoS One 9 (8), e103705.

Landaas, E.T., Storm, M.L., Tollanes, M.C., Barlinn, R., Kran, A.B., Bragstad, K., Christensen, A., Andreassen, T., 2021. Diagnostic performance of a SARS-CoV-2 rapid antigen test in a large, Norwegian cohort. J. Clin. Virol. 137 (104789), 04.

Larsen, D.A., Wigginton, K.R., 2020. Tracking COVID-19 with wastewater, 10 Nat. Biotechnol. 38 (10), 1151–1153, 10.

Li, Michael, Dushoff, Jonathan, Bolker, Benjamin M., 2018. Fitting mechanistic epidemic models to data: a comparison of simple Markov chain Monte Carlo approaches. Stat. Methods Med. Res. 27 (7), 1956–1967.

Li, Q., Guan, X., Wu, P., Wang, X., Zhou, L., Tong, Y., Ren, R., Leung, K.S.M., Lau, E.H.Y., Wong, J.Y., Xing, X., Xiang, N., Wu, Y., Li, C., Chen, Q., Li, D., Liu, T., Zhao, J., Liu, M., Tu, W., Chen, C., Jin, L., Yang, R., Wang, Q., Zhou, S., Wang, R., Liu, H., Luo, Y., Liu, Y., Shao, G., Li, H., Tao, Z., Yang, Y., Deng, Z., Liu, B., Ma, Z., Zhang, Y., Shi, G., Lam, T.T.Y., Wu, J.T., Gao, G.F., Cowling, B.J., Yang, B., Leung, G.M., Feng, Z., 2020. Early transmission dynamics in Wuhan, China, of novel coronavirus-infected pneumonia, 03 N. Engl. J. Med. 382 (13), 1199–1207, 03.

Li, X., Zhang, S., Shi, J., Luby, S.P., Jiang, G., 2021. Uncertainties in estimating SARS-CoV-2 prevalence by wastewater-based epidemiology (Jul). Chem. Eng. J. 415, 129039 (Jul).

Li, X., Kulandaivelu, J., Zhang, S., Shi, J., Sivakumar, M., Mueller, J., Luby, S., Ahmed, W., Coin, L., Jiang, G., 2021 (May). Data-driven estimation of COVID-19 community prevalence through wastewater-based epidemiology 789, 147947 (May).

Lun, J.H., Hewitt, J., Sitabkhan, A., Eden, J.S., EnosiTuipulotu, D., Netzler, N.E., Morrell, L., Merif, J., Jones, R., Huang, B., Warrilow, D., Ressler, K.A., Ferson, M.J., Dwyer, D.E., Kok, J., Rawlinson, W.D., Deere, D., Crosbie, N.D., White, P.A., 2018. Emerging recombinant noroviruses identified by clinical and waste water screening (Mar). Emerg Microbes Infect 7 (1), 50 (Mar).

Mandal, P., Gupta, A.K., Dubey, B.K., 2020. A review on presence, survival, disinfection/removal methods of coronavirus in wastewater and progress of wastewater-based epidemiology (Oct). J. Environ. Chem. Eng. 8 (5), 104317 (Oct).

McLaughlin, Angela, Montoya, Vincent, Miller, Rachel L., Mordecai, Gideon J., Worobey, Michael, Poon, Art F.Y., Joy, Jeffrey B., 2021. Early and ongoing importations of sars-cov-2 in canada. medRxiv.

McMahan, C.S., Self, S., Rennert, L., Kalbaugh, C., Kriebel, D., Graves, D., Deaver, J.A., Popat, S., Karanfil, T., Freedman, D.L., 2020. medRxivCOVID-19 wastewater epidemiology: a model to estimate infected populations (Nov). medRxiv (Nov).

Medema, Gertjan, Heijnen, Leo, Elsinga, Goffe, Italiaander, Ronald, Brouwer, Anke, 2020. Presence of sars-coronavirus-2 rna in sewage and correlation with reported covid-19 prevalence in the early stage of the epidemic in the netherlands. Environ. Sci. & Technol. Lett. 7 (7), 511–516.

Mettler, Sofia K., Kim, Jihoo, Maathuis, Marloes H., 2020. Diagnostic serial interval as a novel indicator for contact tracing effectiveness exemplified with the sars-cov-2/covid-19 outbreak in south korea. Intern. J. Infect. Dis. 99, 346–351.

Michael-Kordatou, I., Karaolia, P., Fatta-Kassinos, D., 2020. J Environ Chem EngSewage analysis as a tool for the COVID-19 pandemic response and management: the urgent need for optimised protocols for SARS-CoV-2 detection and quantification (Oct). J. Environ. Chem. Eng. 8 (5), 104306 (Oct).

K. Mizumoto, K. Kagaya, A. Zarebski, and G. Chowell.Estimating the asymptomatic proportion of coronavirus disease 2019 (COVID-19) cases on board the Diamond Princess cruise ship, Yokohama, Japan, 2020. Euro Surveill, 25(10), 032020.

Murthy, Srinivas, Archambault, Patrick M., Atique, Anika, Martin Carrier, François, Cheng, Matthew P., Codan, Cassidy, Daneman, Nick, Dechert, William, Douglas, Sarah, Fiest, Kirsten M., Fowler, Robert, Goco, Geraldine, Gu, Yusing, Guerguerian, Anne-Marie, Hall, Richard, Hsu, Jimmy M., Joffe, Ari, Jouvet, Philippe, Kelly, Laurel, Kho, Michelle E., Kruisselbrink, Rebecca J., Kumar, Deepali, James Kutsogiannis, Demetrios, Lamontagne, François, Lee, Todd C., Menon, Kusum, O'Grady, Heather, O'Hearn, Katie, Ovakim, Daniel H., Pharand, Scott G., Pitre, Tyler, Reel, Riley, Reeve, Brenda, Rewa, Oleksa, Richardson, David, Rishu, Asgar, Sandhu, Gyan, Sarfo-Mensah, Shirley, Shadowitz, Ellen, Sligl, Wendy, Solomon, Joshua, Stelfox, Henry T., Swanson, Ashleigh, Tessier-Grenier, Hubert, Tsang, Jennifer L.Y., Wood, Gordon, 2021. Characteristics and outcomes of patients with covid-19 admitted to hospital and intensive care in the first phase of the pandemic in canada: a national cohort study. Canadian Med. Assoc. Open Access J. 9 (1), E181–E188.

National Institute for Public Health Netherlands, Welfare the Environment, Ministry of Health, and Sport. Coronavirus monitoring in sewage research. Amsterdam: National Institute for Public Health and the Environment, Mar 2021.

Naughton, C.C., 2020. COVIDPoops19 summary of global SARS-CoV-2 wastewater monitoring efforts by UC merced researchers. ArcGIS Online Dashboard.

Néant, Nadège, Lingas, Guillaume, Hingrat, Quentin Le, Ghosn, Jade, Engelmann, Ilka, Lepiller, Quentin, Gaymard, Alexandre, Ferré, Virginie, Hartard, Cédric, Plantier, Jean-Christophe, Thibault, Vincent, Marlet, Julien, Montes, Brigitte, Bouiller, Kevin, Lescure, François-Xavier, Timsit, Jean-François, Faure, Emmanuel, Poissy, Julien, Chidiac, Christian, Raffi, François, Kimmoun, Antoine, Etienne, Manuel, Richard, Jean-Christophe, Tattevin, Pierre, Garot, Denis, Moing, Vincent Le, Bachelet, Delphine, Tardivon, Coralie, Duval, Xavier, Yazdanpanah, Yazdan, Mentré, France, Laouénan, Cédric, Visseaux, Benoit, Jérémie, Guedj, 2021. Modeling sars-cov-2 viral kinetics and association with mortality in hospitalized patients from the french covid cohort. Proceed. Nat. Acad. Sci. 118 (8).

Nishiura, H., Kobayashi, T., Miyama, T., Suzuki, A., Jung, S.M., Hayashi, K., Kinoshita, R., Yang, Y., Yuan, B., Akhmetzhanov, A.R., Linton, N.M., 2020. Estimation of the asymptomatic ratio of novel coronavirus infections (COVID-19). Int. J. Infect Dis. 94 (154–155), 05.

Ontario Agency for Health Protection and Promotion (Public Health Ontario).COVID-19 overview of the period of communicability ? what we know so far. Toronto, ON. Queenas Printer for Ontario, 2021.

Owusu, Daniel, Pomeroy, Mary A., Lewis, Nathaniel M., Wadhwa, Ashutosh, Yousaf, Anna R., Whitaker, Brett, Dietrich, Elizabeth, Hall, Aron J., Chu, Victoria, Thornburg, Natalie, Christensen, Kimberly, Kiphibane, Tair, Willardson, Sarah, Westergaard, Ryan, Dasu, Trivikram, Pray, Ian W., Bhattacharyya, Sanjib, Dunn, Angela, Tate, Jacqueline E., Kirking, Hannah L., Matanock, Almea, Study Team, Household Transmission, 2021. Persistent SARS-CoV-2 RNA shedding without evidence of infectiousness: a cohort study of individuals with COVID-19. J. Infect. Dis. 02 jiab107.

Paglinawan, Denise, 2020. University of Guelph testing campus residences' wastewater to detect COVID-19 (Oct). CBC News - The Canadian Press (Oct).

Peccia, J., Zulli, A., Brackney, D.E., Grubaugh, N.D., Kaplan, E.H., Casanovas-Massana, A., Ko, A.I., Malik, A.A., Wang, D., Wang, M., Warren, J.L., Weinberger, D. M., Arnold, W., Omer, S.B., 2020. Measurement of SARS-CoV-2 RNA in wastewater tracks community infection dynamics, 10 Nat. Biotechnol. 38 (10), 1164–1167, 10.

Pecson, Brian M., Darby, Emily, Haas, Charles N., Amha, Yamrot M., Bartolo, Mitchel, Danielson, Richard, Dearborn, Yeggie, Giovanni, George Di, Ferguson, Christobel, Fevig, Stephanie, 2021. Reproducibility and sensitivity of 36 methods to quantify the sars-cov-2 genetic signal in raw wastewater: findings from an interlaboratory methods evaluation in the us. Environ. Sci.: Water Res. Technol. 7 (3), 504–520.

Peiser, Jaclyn, 2020. University of Arizona used wastewater testing to detect cases of coronavirus in a dorm (Aug). The Washington Post (Aug).

Public Health Ontario.Ontario Agency for Health Protection and Promotion, Wastewater surveillance of COVID-19, Toronto, ON. Queenas Printer for Ontario, Apr 2021b.

Public Health Ottawa.Wastewater COVID-19 surveillance. Ottawa Public Health, Ontario, Canada, 2021a.

Rabson, Mia, 2021. Researchers looking for clues to the COVID-19 pandemic in city sewers (Apr). Global News, The Canadian Press (Apr).

Randazzo, W., Truchado, P., Cuevas-Ferrando, E., Simon, P., Allende, A., Sanchez, G., 2020. SARS-CoV-2 RNA in wastewater anticipated COVID-19 occurrence in a low prevalence area (Aug). Water Res. 181, 115942 (Aug).

Reynolds, Matthew W., Xie, Yiqiong, Knuth, Kendall B., Mack, Christina D., Brinkley, Emma, Toovey, Stephen, Dreyer, Nancy A., 2022. Covid-19 vaccination breakthrough infections in a real-world setting: using community reporters to evaluate vaccine effectiveness. medRxiv.

Rizzo, L., Manaia, C., Merlin, C., Schwartz, T., Dagot, C., Ploy, M.C., Michael, I., Fatta-Kassinos, D., 2013. Urban wastewater treatment plants as hotspots for antibiotic resistant bacteria and genes spread into the environment: a review (Mar). Sci. Total Environ. 447, 345–360 (Mar).

Rousis, N.I., Zuccato, E., Castiglioni, S., 2016. Monitoring population exposure to pesticides based on liquid chromatography-tandem mass spectrometry measurement of their urinary metabolites in urban wastewater: a novel biomonitoring approach (Nov). Sci. Total Environ. 571, 1349–1357 (Nov).

Rousis, N.I., Zuccato, E., Castiglioni, S., 2017. Wastewater-based epidemiology to assess human exposure to pyrethroid pesticides (Feb). Environ. Int. 99, 213–220 (Feb).

Sayampanathan, A.A., Heng, C.S., Pin, P.H., Pang, J., Leong, T.Y., Lee, V.J., 2021. Infectivity of asymptomatic versus symptomatic COVID-19, 01 Lancet 397 (10269), 93–94, 01.

Silverman, Andrea I., Boehm, Alexandria B., 2020. Systematic review and meta-analysis of the persistence and disinfection of human coronaviruses and their viral surrogates in water and wastewater, 08 Environ. Sci. Technol. Lett. 7 (8), 544–553, 08.

Sims, N., Kasprzyk-Hordern, B., 2020. Future perspectives of wastewater-based epidemiology: Monitoring infectious disease spread and resistance to the community level 139 (105689), 06.

Statistics Canada.2016 Census of Canada via Toronto Public Health.2016.

Tian, Di, Lin, Zhen, Kriner, Ellie M., Esneault, Dalton J., Tran, Jonathan, DeVoto, Julia C., Okami, Naima, Greenberg, Rachel, Yanofsky, Sarah, Ratnayaka, Swarnamala, Tran, Nicholas, Livaccari, Maeghan, Lampp, Marla, Wang, Noel, Tim, Scott, Norton, Patrick, Scott, John, Hu, Tony Y., Garry, Robert, Delafontaine, Patrice, Hamm, Lee, Yin, Xiao-Ming, 2021. Sars-cov-2 load does not predict transmissibility in college students. medRxiv.

Topol, Eric J., Oran, Daniel P., 2021. The proportion of sars-cov-2 infections that are asymptomatic. Annals of Intern. Med. 174 (5), 655–662. PMID: 33481642.

Toronto Water.City of Toronto, Ashbridges Bay wastewater treatment plant annual report of 2020. Online, 2021a.

Toronto Water.City of Toronto, Highland Creek wastewater treatment plant annual report of 2020. Online, 2021c.

Toronto Water.City of Toronto, Humber wastewater treatment plant annual report of 2020. Online, 2021b.

Wang, Kun, Zhang, Xin, Sun, Jiaxing, Ye, Jia, Wang, Feilong, Hua, Jing, Zhang, Huayu, Shi, Ting, Li, Qiang, Wu, Xiaodong, 2020. Differences of severe acute respiratory syndrome coronavirus 2 shedding duration in sputum and nasopharyngeal swab specimens among adult inpatients with coronavirus disease 2019. Chest 158 (5), 1876–1884.

Wearing, Helen J., Rohani, Pejman, Keeling, Matt J., 2005. Appropriate models for the management of infectious diseases. PLoS Med. 2 (7), e174.

Weidhaas, J., Aanderud, Z.T., Roper, D.K., VanDerslice, J., Gaddis, E.B., Ostermiller, J., Hoffman, K., Jamal, R., Heck, P., Zhang, Y., Torgersen, K., Laan, J.V., LaCross, N., 2021. Correlation of SARS-CoV-2 RNA in wastewater with COVID-19 disease burden in sewersheds (Jun). Sci. Total Environ. 775, 145790 (Jun).

WHO.World Health Organization, Status of environmental surveillance for SARS-CoV-2 virus: scientific brief. World Health Organization, 2020.

Wurtzer, S., Marechal, V., Mouchel, J.M., Maday, Y., Teyssou, R., Richard, E., Almayrac, J.L., Moulin, L., 2020. Evaluation of lockdown effect on SARS-CoV-2 dynamics through viral genome quantification in waste water, Greater Paris, France, 5 March to 23 April 2020, 12 Euro Surveill 25 (50), 12.

Xiao, A., Wu, F., Bushman, M., Zhang, J., Imakaev, M., Chai, P.R., Duvallet, C., Endo, N., Erickson, T.B., Armas, F., Arnold, B., Chen, H., Chandra, F., Ghaeli, N., Gu, X., Hanage, W.P., Lee, W.L., Matus, M., McElroy, K.A., Moniz, K., Rhode, S.F., Thompson, J., Alm, E.J., 2021. medRxivMetrics to relate COVID-19 wastewater data to clinical testing dynamics (Jun). medRxiv (Jun).

Yewdell, J.W., 2021. Individuals cannot rely on COVID-19 herd immunity: durable immunity to viral disease is limited to viruses with obligate viremic spread, 04 PLoS Pathog. 17 (4), e1009509, 04.

Zhu, Y., Oishi, W., Maruo, C., Saito, M., Chen, R., Kitajima, M., Sano, D., 2021. Early warning of COVID-19 via wastewater-based epidemiology: potential and bottlenecks (May). Sci. Total Environ. 767, 145124 (May).

Zuccato, E., Chiabrando, C., Castiglioni, S., Calamari, D., Bagnati, R., Schiarea, S., Fanelli, R., 2005. Cocaine in surface waters: a new evidence-based tool to monitor community drug abuse (Aug). Environ. Health 4 (14) (Aug).

Zuccato, E., Chiabrando, C., Castiglioni, S., Bagnati, R., Fanelli, R., 2008. Estimating community drug abuse by wastewater analysis (Aug). Environ. Health Perspect 116 (8), 1027–1032 (Aug).